000

415001

PART 1

ASPECTS OF THE TENTH LEGION SKARN, NORTH-WEST TASMANIA

---

by

Donald F. Thomson

Part 1 of

A thesis in two parts submitted in partial fulfilment of the requirements for the Degree of Bachelor of Science with Honours (Geology)

November 1983

LATROBE UNIVERSITY,
BUNDOORA, VIC.

001

415002

TABLE OF CONTENTS

ABSTRACT

Petrographic studies have shown the Tenth Legion deposit to be a tin-bearing magnetite magnesian skarn in which the magnetite and sulphide mineralisation is associated with serpentinisation of the forsterite, diopside, and tremolite of the primary ore skarn. Previous studies have suggested that this deposit formed as a result of the alteration of an ultramafic body. However this interpretation is not supported by microprobe and EDAX analyses obtained during this study. The alternative interpretation advanced here is that the deposits formed during metasomatism by Fe, SiO_2 and S-bearing fluids.

A number of alteration stages are recognised in the Tenth Legion skarn. During the principal alteration stage various calcic and magnesian silicates were formed by the contact metamorphism and metasomatic alteration of dolomites. Metamorphic grades ranging from albite-epidote-hornfels facies to pyroxene-hornfels facies are indicated by stable mineral assemblages. Temperatures during Stage II alteration were between 350-550°C. In other skarns containing serpentine alteration the serpentinisation is regarded as belonging to the post ore stage, but at Tenth Legion is considered to have occurred contemporaneously with serpentinisation.

005

1 INTRODUCTION

1.1 General

Tenth Legion is a tin-bearing magnesium skarn deposit located in North-West Tasmania (Fig.1). It differs from the other carbonate replacement deposits in this region, Renison Bell, Mt. Bischoff, Cleveland and Razorback (Hall and Solomon 1962), in that the tin mineralisation is associated with magnetite rather than massive sulphides.

Over two hundred magnetite-magnesium skarns are known from around the world and many of these are associated with economic tin mineralisation (Shabynin 1971). However, the majority of these deposits are only poorly described in Western literature. An extensive literature search suggests that Tenth Legion has similarities to some Russian deposits e.g. Kitelya (Materikov 1977), but, as far as is known, the interpretation advanced here differs significantly from that in previously published studies.

1.2 Scope of Present Study and Methods

The purpose of this study was to describe the nature and origin of mineralisation at Tenth Legion and to characterise the alteration sequence and any zonation within the deposit. This involved the detailed petrographic study of representative core samples, combined with SEM and microprobe analysis of selected samples. The deposit was not mapped, but an inspection of the site and the adjacent Heemskirk Granite was carried out.

006

415007

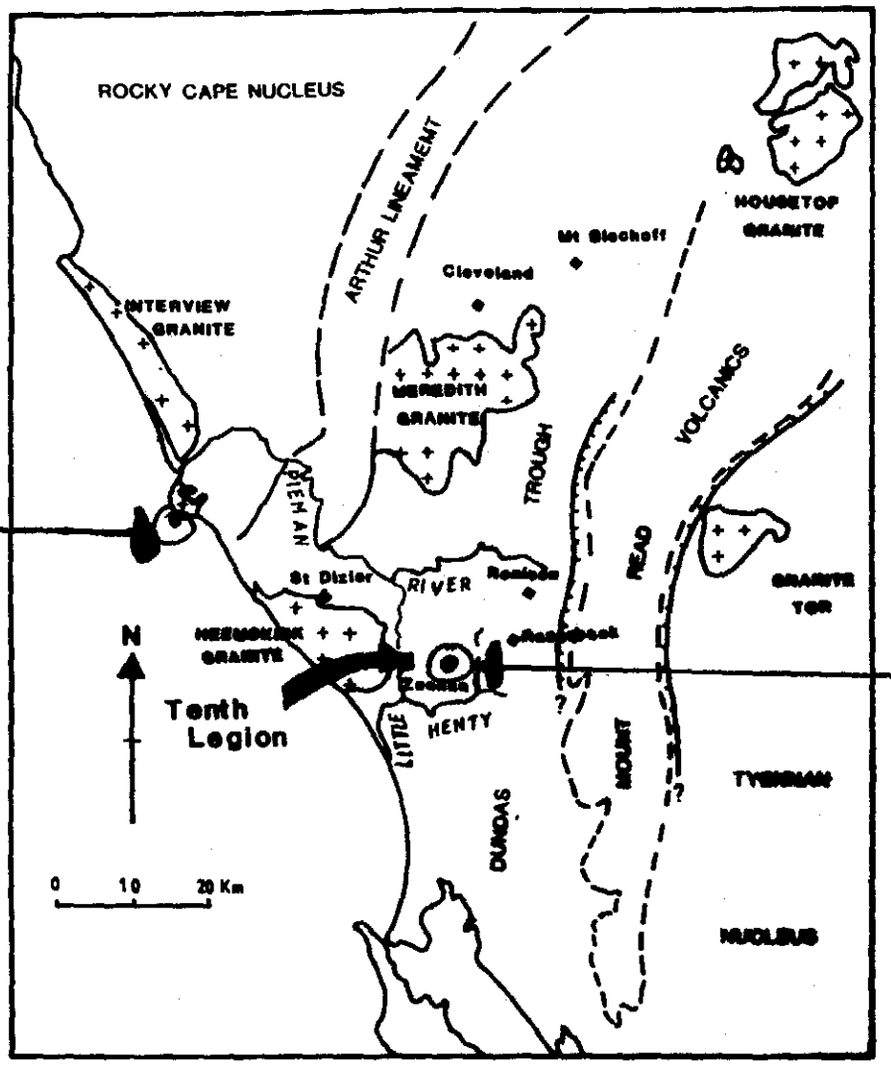

AMG
337500E
5368800N

AMG
362000E
5362000N

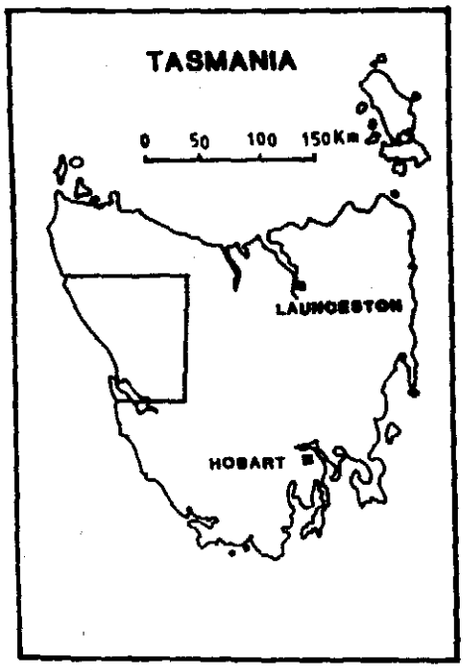

Devonian Granite

Original Limit
Mt Read Volcanics

Outcrop
Mt Read Volcanics

Tin-sulphide Deposit

5 cm

Fig: 1

AMG REFERENCE POINTS ADDED

007

1.3 Location and Access

Tenth Legion is situated at the base of Mt. Agnew, 12 km west of Zeehan, Western Tasmania (Fig.1). Access is via the Trial Harbour Road to Comstock, from where a 4-wheel drive track branches off to the northwest. This track is badly eroded, and would only be passable in dry weather.

1.4 Topography

With the exception of Mt. Agnew, the country around the Tenth Legion deposit is gently undulating and is largely covered by button grass. Mt. Agnew, to the west of the deposit, is part of the Heemskirk Granite and rises to a height of 844 metres. The deposit itself is covered by dense vegetation and is intersected by a series of small gullies which form a dendritic drainage pattern. These gullies form the upper reaches of Pine Creek, which flows north before joining the Pieman River (Fig.1), and Kynance Creek which flows south to the Little Henty River.

1.5 Previous Work

The Tenth Legion deposit has been known since 1885 (Blissett 1962), and was prospected for silver and lead, by the Tenth Legion Company, between 1901 and 1902. Waller (1903) considered the deposit to be part of the contact aureole around the Heemskirk Granite which was assumed to be the source of the mineralisation.

The deposit was mentioned in reports by Twelvetrees (1901), Ward (1910) and Waterhouse (1916). From 1920-1936 G. and C.

008

Hoskins (Hoskins Iron & Steel) excavated 17 adits and several costeens at Tenth Legion. Australian Iron & Steel subsequently took over the leases with a view to mining the iron ore. Blake (1928) described the deposit in a report on the iron ore reserves of Tasmania. In an official government report in 1939, Woolnough recommended that thorough mapping and sampling of the deposit be undertaken. This work was carried out by Blake (1940) and included assays for iron and estimates of reserves.

The Tasmanian Department of Mines undertook further work and sank two diamond drill holes into the northern magnetite lens. In his report on this work Hughes (1959) suggested that the deposit formed as the result of metasomatic alteration of Cambrian gabbros. He based this interpretation on the similarities to the Savage River deposit which is associated with basic and ultrabasic igneous rocks. Blissett (1962) briefly mentioned the deposit in his report on the Zeehan area and incorrectly mapped it as an ultrabasic intrusive. Both and Williams (1968) also considered the deposit to be related to the Cambrian intrusives.

The most recent work at Tenth Legion was carried out by C.R.A. The company mapped the deposit in detail and sank 14 diamond drill holes. The drill core was assayed for Cu, Zn, Pb, Sn and W. The present study is based on the C.R.A. material.

009

REGIONAL GEOLOGY

The Tenth Legion skarn is confined to the contact aureole of the Heemskirk Granite (Inset Map 1). The granite intrudes a Proterozoic sequence of quartzites, siltstones, shales and dolomites, which constitute the Oonah Quartzite and Slate (Blissett 1962). The Proterozoic sequence is conformably overlain by the Success Creek Group, an Early Cambrian succession of volcanics, shales, quartzites and carbonates (Corbett and Brown 1976) which underly the Cambrian sediments in the Dundas Trough (Solomon 1981).

The Proterozoic sequence contains Late Cambrian gabbros and peridotites. Minor nickel and chromium mineralisation are associated with the ultramafics (Corbett and Brown 1976). The Late Cambrian to Silurian is characterised by unconformable detrital sedimentation. The dominant lithologies are conglomerates, sandstones and fossiliferous limestones (Blissett 1962). Sedimentation was interrupted by the widespread Tabberabberan Orogeny during the Mid-Devonian (Blissett 1962, Corbett and Brown 1976, Solomon 1981). The Heemskirk Granite was intruded during this period of instability. The granite has been dated at 354 my (Rb-Sr total rock) by Brooks and Compston (1965), who postulated a crustal source to explain the extremely high initial Rb-Sr ratios of the granite. The Heemskirk Granite is considered to be responsible for the extensive mineralisation at Zeehan, but the exact relationship between the granite and various ore bodies is not well understood (Both and Williams

010

1968, Solomon 1981).

Erosion occurred throughout the Carboniferous and was followed by glacial, freshwater and marine deposition during the Permian. Scattered outliers of the Permian deposits occur around the Zeehan district and near Mt. Read (Blissett 1962). Limited igneous activity occurred in the region during the Jurassic when the dolerite which now forms Mt. Dundas was intruded. Non-marine sediments were deposited during the Cainzoic and some igneous activity occurred around Granville Harbour (Blissett 1962) during this time.

3 LOCAL GEOLOGY

3.1 Heemskirk Granite

The Heemskirk Granite lies outside of the prospect area held by C.R.A. and could not be studied in detail because the granite and immediate contact around Mt. Agnew was held by Renison-Goldfields Ltd. at the time. The albitised margin of the granite was examined because of the likelihood of granite playing a role in the formation of Tenth Legion.

The granite is an elliptical body with an outcrop area of 119 km^2 which intrudes and is almost completely enclosed within the Oonah Quartzites. It was sub-divided into three phases, White Granite A, White Granite B and Red Granite by Brooks and Compston (1965). The Red Granite occurs around Mt. Agnew where it has been albitised.

011

The nearest granite outcrop is about 600 m from Tenth Legion. It contains rounded plagioclase and quartz phenocrysts, up to 10 mm across, in a medium grained matrix. The plagioclase phenocrysts are pale green in colour and are surrounded by bluish coloured "reaction" rims. In contrast to the larger phenocrysts, the smaller plagioclases are tabular and white. Tourmaline clots, up to 50 mm across, stud the weathered surface of the granite (Fig.3). Anhedral purple fluorite grains up to 1 mm across are also present and pyrite occurs within small mirolitic cavities.

Thin section examination reveals that the granite is composed of perthitic K-feldspar, plagioclase and quartz. Two types of plagioclase can be distinguished: (1) zoned plagioclase whose cores are almost completely replaced by sericite, and (2) unzoned albite - obligoclase (An_5 - An_{15}). Large fluorite inclusions up to 1 mm across occur within the plagioclases. The margins of the larger felsic minerals are rounded and often interlocking. The fabric has an aplitic texture which borders on granophyre. The K-feldspar is only mildly sericitised and has a brown, cloudy appearance in plane polarised light. The only mafic mineral is chloritised biotite (α = khaki, $\beta = \gamma$ = brown). Biotite clots frequently contain secondary sphene, tourmaline, secondary fluorite and occasionally cassiterite. The fluorite has developed parallel to the cleavage in the biotite.

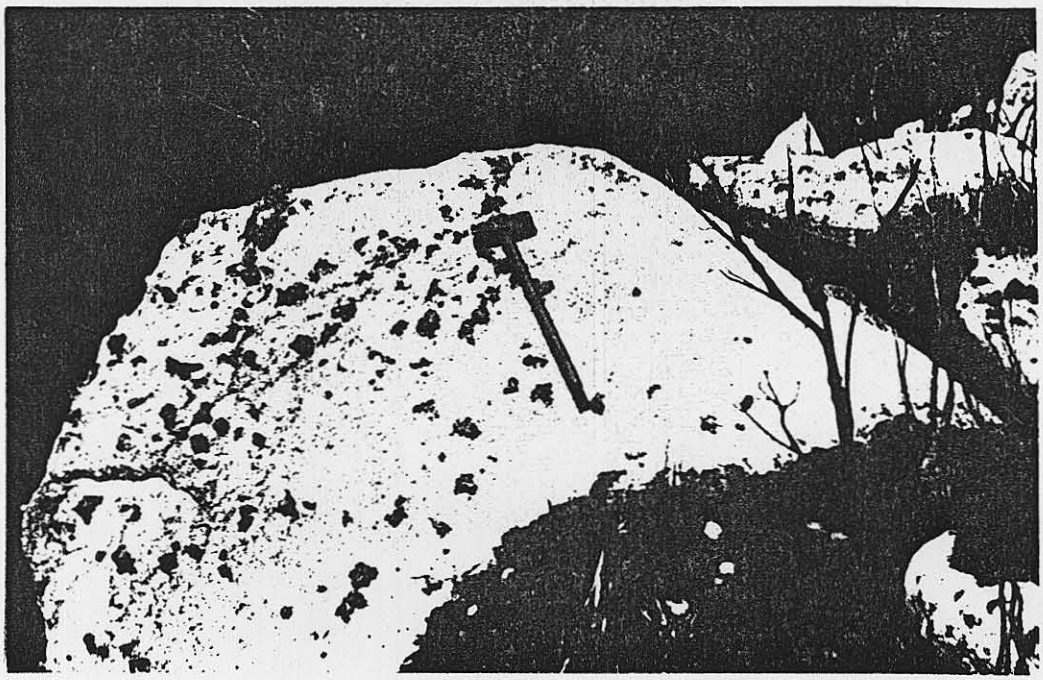

Fig. 3 Typical outcrop of the Heemskirk Granite with tourmaline clots in weathered surface.

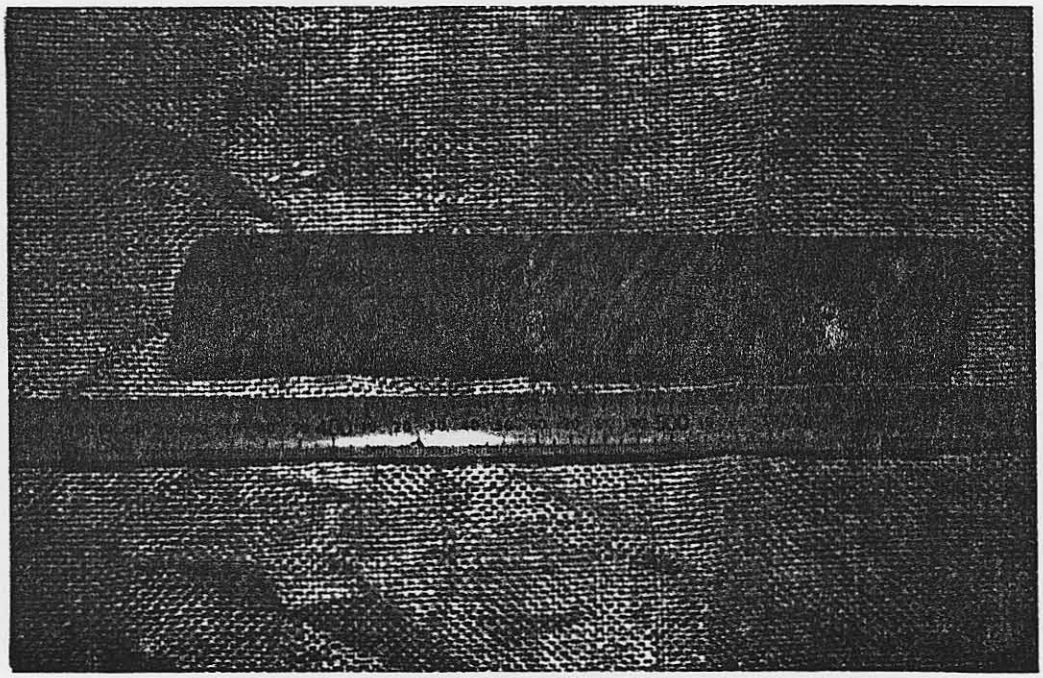

Fig. 4 Metasomatised hornfels with tourmaline alteration.

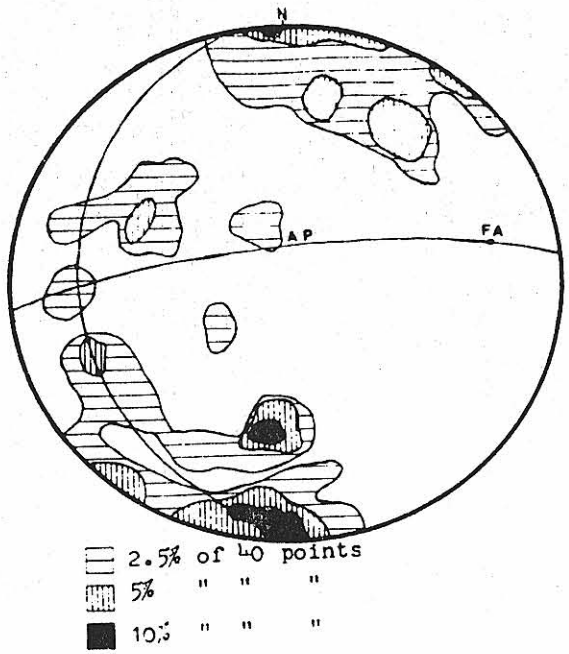

Fig. 5 Stereo net of poles to bedding. The dominant structure is a tightly folded antiform. Fold axis (FA) orientation 54° 060°. Approximate axial plane (AP) 078/88NW.

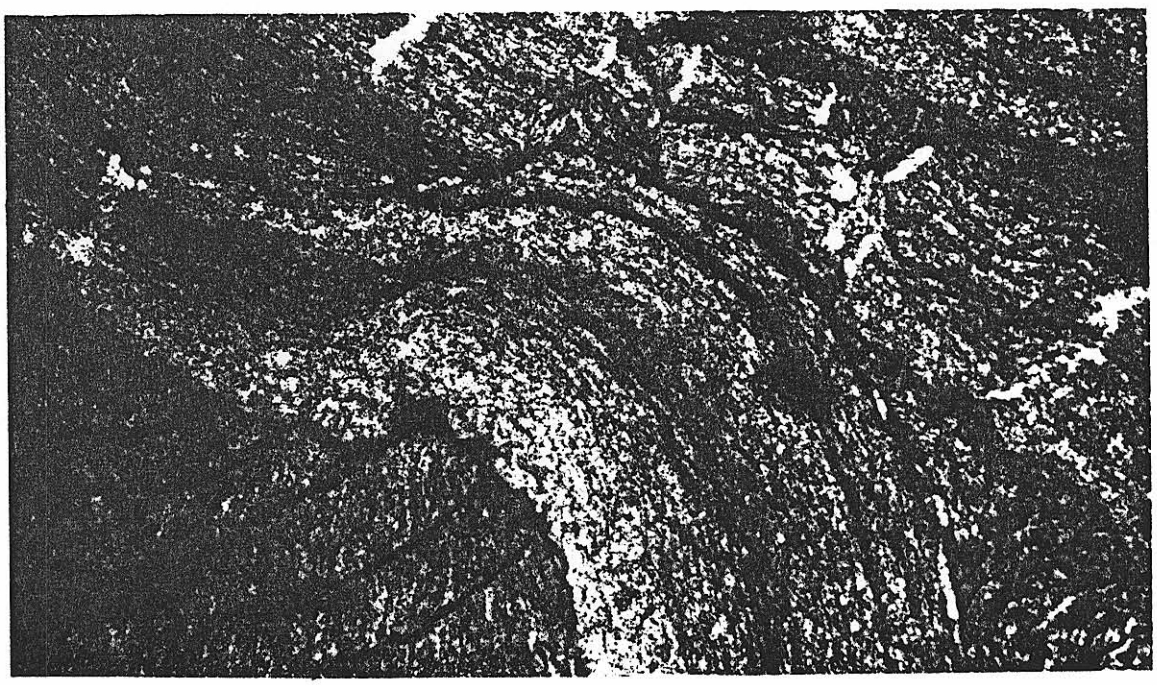

Fig. 6 Photomicrograph of folded foliation (S_1) (parallel to layering). Parasatic crenulations have developed in the hinge of the larger fold. (Plane polarised light).

014

3.2 Gabbro

Gabbro occurs to the east of the deposit, but most of the outcrop is outside the lease area and the unit was not intersected by any of the diamond drill holes drilled by C.R.A. Only a cursory examination of this unit was made in the field for the purposes of comparison with the pyroxene and serpentine-bearing skarns.

The gabbro outcrops as both flat lying sheets and large jointed boulders. It is massive, medium grained and green in colour (LTU 6720). It consists of altered clinopyroxene and hornblende with minor relict plagioclase. The clinopyroxenes and amphiboles are chloritised and serpentinised. The plagioclase is largely sericitised. Despite the severe alteration,the interlocking nature of the primary fabric is preserved.

3.3 Sedimentary Host Rocks

The sedimentary host rocks consist of metamorphosed quartzite, siltstone, shale and carbonate units. Many of the more massive horizons can be correlated between adjacent drill holes (Fig.2). The comparison of units is complicated by brecciation, preferential replacement of units, and varying degrees of alteration. Consequently, many of the thinner units are laterally discontinuous.

The following discussion is a list of the dominant rock types after metamorphism. The order of listing does not have any stratigraphic significance.

3.3.1 Hornfels

Two distinct types of hornfels are recognised: (1) metaquartzites and siltstones, and (2) black shales. The metaquartzites and siltstones consist of finely laminated, quartz-rich layers which alternate with micaceous bands. Grain size varies from 0.001 mm to 1 mm. The more coarse grained examples are massive. The metaquartzites consist mainly of quartz grains which frequently exhibit undulose extinction and have interlocking, sutured boundaries. Composite grains have been recrystallised to fine, granular mosaics which pseudomorph the original grains. In addition to quartz, fine, white mica, diopside, tremolite (T.S. 9 - 147.9* and T.S. 2 - 49.2) and epidote (T.S. 2 - 19.5) are present. Some sections (e.g. T.S. 11 - 100.1 and T.S. 14 - 134), have undergone extensive metasomatic tourmalinisation (Fig.4) and contain 15 - 20% dravite. The tourmaline tends to preferentially replace micaceous horizons. Altered cordierite prophyroblasts occur in the spotted hornfels (T.S.2 - 125.7).

In contrast to the metaquartzites and siltstones, the black shales consist of alternating micaceous and graphitic bands. The micaceous laminae are very fine grained and the exact mineralogy could not be determined. Relict porphyroblasts (? andalusite; <1 mm across) occur in the pelitic layers in T.S. 2 - 39.2.

* T.S. = thin section

016

3.3.2 Tourmalisation of Hornfels

Dravite occurs in varying amounts in both types of hornfels. It is particularly abundant in thin sections 14 - 134, 10 - 97.6 and 11 - 100.1, where it appears to be replacing, but not pseudomorphing,aluminous phases such as mica and cordierite.

3.3.3 Carbonate

The carbonates are usually dolomitic breccias. The cause of brecciation is not known. During low grade contact metamorphism, the carbonates were recrystallised to massive dolomitic marbles. Staining has shown these marbles to be a combination of dolomite and calcite, with dolomite predominating. Grain boundaries are distinct and clear cut. Grain size varies from less than 1 mm up to 5 mm. Some specimens of drill core have a light, dirty grey colour which is due to the presence of fine, dusty magnetite and carbonaceous material. Calcic and magnesium contact metamorphic skarns occur where the carbonates have been in contact with quartz and pelitic beds (see section 4).

3.4 Structure

The host rocks at Tenth Legion have undergone at least two deformations. The structural complexity of the area is illustrated by Fig.5 which shows poles to bedding. This stereo net is a compilation of data from the C.R.A. map of the area. The dominant feature shown by the plot is a tightly folded antiform which plunges at 54^{o} towards 060^{o}. The approximate axial plane has an orientation of 078/88NW. The fold axis which occupies the

017

central portion of Map 1, has a similar orientation to other regional structures (Inset Map 1). The correlation of lithologies on opposite limbs of the fold axis is poor because of the limited number of drill holes.

Two deformations are evident from structures observed in the hornfels units. The earliest of the deformation is represented by a foliation (slaty cleavage) developed at a low angle to the dominant planar lamination (probably bedding) e.g. T.S. 2 - 39.2. The second deformation is typified by asymmetric kinks which overprint the earlier foliation (T.S. 12 - 58.45 and 11 - 100.1). These two samples came from widely spaced drill holes and have the same style of field. The kinks have rounded to angular hinges. Micaceous laminae have been deformed around the hinges in a ductile manner and have developed parasitic crenulations within the cores of the larger kinks (Fig. 6).

The skarn assemblages do not have any tectonic overprint and must therefore post-date deformation. If the formation of the skarn accompanied granite intrusion, the deformations must also predate the emplacement of the Heemskirk Granite.

Faulting on a regional scale occurred along the Tenth Legion Fault (Inset Map 1) and local faulting is evident from the drill hole data although the sense of movement is unknown. The evidence for faulting in the drill core is the presence of localised breccias and the poor correlation of otherwise continuous units between adjacent drill holes (See Fig.2, nos. 11 and 14).

018

4 SKARNS

The term "skarn" refers to the calcium and magnesium silicates associated with ore deposits (Burt 1977). Skarns can be divided into two types, ore skarn and contact metamorphic skarn (Kwak and Askins,1981), which differ in the mode of their formation and the composition of their minerals. Metamorphic skarn (also called bimetasomatic and reaction skarn) is produced by local exchange of silica, calcium and magnesium between adjacent carbonate and silica horizons, or by the metamorphism of marly units (Kwak and Askins,1981). Replacement skarn is produced by the reaction of quartz-free carbonate rocks with hydrothermal solutions which may introduce Fe, Si and some or all of the following, Cu, Pb, Zn, Sn, W, Be, F, U and S to the carbonates. The replacement skarn may be distinguished from the contact metamorphic skarn by the presence of these elements in anomalously high concentrations. Metallic ores can occur in the replacement skarn to the virtual exclusion of silicates. In such cases the term "ore skarn" is a more appropriate term. Similarly, the predominance of silica and Al-rich, Fe-poor phases, such as grossular, instead of andradite garnet, serves to distinguish the contact skarn from the replacement skarns (Kwak and Askins, 1981).

Using these definitions a number of primary replacement and contact assemblages can be recognised at Tenth Legion. The contact assemblages are shown in Table 1 and the ore skarn assemblages

019

in Table 2. The contact metamorphic and replacement assemblages represent two extremes in a continuum and mixtures of these assemblages do occur.

4.1 Contact Metamorphic Skarn

The assemblages in the first column of Table 1 appear to be stable on the basis of petrographic evidence. Extensive hydrothermal alteration has occurred throughout the deposit and many of the contact minerals have been replaced by hydrous phases (Table 1). This is most evident in the silica deficient and hydrous assemblages such as those containing olivine and talc.

4.1.1 Magnesium Contact Metamorphic Skarn

Talc-calcite-dolomite

In the distal parts of the deposit, talc replaces dolomite marbles and breccias, producing the assemblage talc-calcite-dolomite. Only a few examples (e.g. T.S. 2 - 95) of this assemblage were found as talc is usually replaced by late-stage γ - serpentine (chrysotile) veins. Classification of the serpentine minerals (Appendix 1) follows the proceedure of Wicks and Whittaker (1977). Magnetite may also be introduced at this stage (Fig.7). The serpentine is often subsequently replaced by carbonate.

TABLE 1 PROBABLE STABLE CONTACT METAMORPHIC SKARN ASSEMBLAGES

	PRINCIPAL STABLE ASSEMBLAGES	ALTERATION AND ADDITIONAL PHASES NOT NECESSARILY IN EQUILIBRIUM	THIN SECTION EXAMPLE
MAGNESIAN SKARN	Ta - Cc - Do	Serp + minor magnetite introduced during alteration	T.S. 2-95
	Ta - Tr - Cc*		
	Fo - Di - Cc*	Not in contact metamorphic skarn found at Tenth Legion	
	Fo - Di - Tr*		
	Di - Tr (Transitional)*		
	Di - Tr - Qtz	Fh - serp (only minor assemblage)	T.S. 9-44
	Ph - Di - Tr	In micaceous layers in siltstone *minor assemblages*	T.S. 2-94.9
CALCIC SKARN	Wol - Di - Cc	Serp + vesu Ep + Cc	T.S. 3-77.6
	Wol - Di - Qtz	Ep - Pl - Cc - Ch	T.S. 2-97.5
	Wol - Di	Serp - Ep - Ch	T.S. 10-55.8
	Wol - Di - Vesu	Ep - Fh - Ch - Ph	T.S. 5-22.3
	Wol - Di - Ga - (?Gr)		T.S. 3-28.5
	Di - Gr - An		T.S. 5-105.44

* Assemblage not identified as being of undisputable contact origin (i.e. also found in ore skarn)

An = Anorthite, Cc = Calcite, Ch = Chlorite, Di = Diopside, Ep = Epidote, Fh = Ferrohastingsite, Ga = Garnet, Gr = Grossolar, Ph = Phlogopite, Pl = Plagioclase, Qtz = Quartz, Serp = Serpentine, Ta = Talc, Vesu = Vesuvianite, Wol = Wollastonite, Do = Dolomite.

TABLE 2

ORE SKARN ASSEMBLAGES

STAGE		MAGNESIAN ORE SKARN	CALCIC ORE SKARN
PROGRESSIVE HYDROUS ALTERATION	I	Ta - Cc - Dol + Mag; Fo - Cc - Dol + Mag; Fo - Di - Cc + Mag; Fo - Di - Tr + Mag; Di - Tr + Mag	Di - And
		& OR; Minor; Sph, Chalco, Py	Serpentine
	IIa	Lizard & or chrysolite	
		Main Magnetite Stage	Further
		Late Fe - Zn - Cu sulphide	Alteration
	IIb	Antigorite	Unknown
	III	Tr / Ta / Chl	Presumed
	IV	Potassic alteration	To Be
		(K - Al ± F ± B Added)	Epidote
		Phlogopite overprints all earlier assemblages - most pronounced near granite contact. Fibrous magnetite formed but replaced by pyrite	Chlorite
	V	Late stage/low temperature overprinting F by calcite & siderite	
		chrysotile veins in serpentine rocks & marbles	

An assemblage may be affected by all or only few stages of alteration.

And = andradite, Cc = calcite, Chalco = chalcopyrite, Chl = chlorite,
Di = diopside, Do = dolomite, Mag = magnetite, Py = pyrite,
Sph = sphalenite, Ta = talc, Tr = tremolite.

022

Forsterite

Stable forsterite assemblages were found at Tenth Legion, but none could be classed as being of contact metamorphic origin according to the strict definitions used here (Mulligan 1968).

Diopside-tremolite-quartz

The assemblage diopside-tremolite-quartz is a silica-saturated product that may form from the reaction of dolomite with excess quartz. This assemblage is found only as a minor component in some quartzites and siltstones. In some cases the diopside alters to ferrohastingsite (T.S. 9 - 44). Reaction between dolomite and argillaceous sediments results in diopside-tremolite-quartz$^{\pm}$phlogopite assemblages (T.S. 2 - 94.9).

4.1.2 Calcic Contact Metamorphic Skarn

Reaction between magnesium marbles and silica-rich units has produced a number of calcic assemblages that are distinct from both magnesian contact metamorphic skarn and the replacement skarn (Table 1). The contact metamorphic calcic assemblages can be divided into two mineralogically distinct groups (Table 1).

Wollastonite-Diopside

The assemblage wollastonite-diopside-quartz is the calcic equivalent of the assemblage diopside-tremolite-quartz in the magnesian contact metamorphic skarn. Samples containing this assemblage may also contain epidote, plagioclase, K-feldspar or garnet (T.S. 2 - 97.5) but these phases appear to be in

023

disequilibrium with diopside-wollastonite-quartz.

Vesuvianite-garnet

The assemblages wollastonite-diopside-vesuvianite (T.S. 5 - 22.3), wollastonite-diopside-garnet (?grossular) (T.S. 3 - 28.5) and diopside-grossular-anorthite (T.S. 5 - 105.45) form where argillaceous sediments (now hornfels) have reacted with magnesian limestones (marbles). Only the example of the first assemblage shows clear evidence of equilibrium relationships.

4.2 Ore Skarn Assemblages

A number of magnesium and calcic ore skarn assemblages and their alteration products occur at Tenth Legion (Table 2). Magnetite, sphalerite, chalcopyrite, pyrite and pyrrhotite can occur as minor additional phases in the primary silicate assemblages. The bulk of the ore mineralisation is, however, associated with the hydrous alteration of earlier formed silicate assemblages (see Section 6).

4.2.1 Magnesium Ore Skarns

Talc

The assemblage talc-calcite-dolomite-magnetite was found in a number of intersections, particularly in the more distal parts of the deposit. The talc may replace dolomite marbles (T.S. 6 - 112). This assemblage can be differentiated from similar assemblages in the contact metamorphic skarn by the presence of magnetite. The talc is usually replaced by late stage $\bar{\gamma}$ - serpentine veins (probably chrysotile). Additional magnetite is introduced when

the talc is replaced by the late-stage chrysotile veins. The magnetite tends to form a network of fine threads along the margins of the serpentine veins. The serpentine is often recrystallised to antigorite or replaced by carbonate during a later event. The sequence is shown in Table 2. No evidence was found of talc altering to forsterite, diopside or tremolite in the initial stages of ore skarn formation.

Forsterite

Three stable forsterite-bearing assemblages are recognisable at Tenth Legion (Table 2). The first of these is the assemblage forsterite-calcite-dolomite-magnetite (T.S. 13 - 76.8). The forsterite in this assemblage occurs as discrete anhedral crystals within massive calcite-dolomite marbles. Magnetite always occurs in the marbles with the forsterite. Serpentine frequently occurs along fractures in the olivine and in the most advanced stages of alteration, completely replaces the olivine.

The forsterite-diopside-calcite assemblage is also confined to massive marbles. Tremolite is sometimes found with this assemblage (T.S. 7 - 24.5) but has textures which are suggestive of disequilibrium (Fig.8). This enables it to be distinguished from the stable assemblage forsterite-diopside-tremolite.

Fresh tremolite was found as fine needles in olivine (T.S. 13 - 106) which suggest that forsterite and tremolite form stable assemblages (Fig.9). Diopside also occurs in equilibrium with forsterite in the same thin section. This gives rise to the

stable assemblage forsterite-diopside-tremolite (Fig.10). A thin band of magnetite occurs along the carbonate-silicate interface in T.S. 13 - 106. This mode of occurrence is typical of early magnetite throughout the deposit.

Diopside-tremolite

The last of the primary magnesium skarn assemblages consists of diopside-tremolite-magnetite. Massive units of this assemblage were intersected by a number of drill holes (Fig.3). In thin section (T.S. 2 - 30) diopside laths form an interlocking framework with finer tremolite. Magnetite occurs as irregular interstitial patches.

4.2.2 Calcic Ore Skarns

Diopside-andradite-calcite

In direct contrast to the situation observed in the magnesium ore skarns, only one calcic assemblage of replacement origin, diopside-andradite-calcite (Fig.11), was identified in the calcic ore skarn. The garnet was identified as andradite from microprobe data (Appendix II). This suggests that the assemblage is of replacement origin because of its high iron content.

Thin sections 13 - 70.6 and 13 - 69.8 are the only examples positively identified as belonging to this assemblage. Thin section 13 - 70.6 basically consists of massive andradite with fine, granular diopside inclusions. Late-stage serpentine veins are partially replaced by calcite. Primary calcite occurs interstitial to the diopside and garnet.

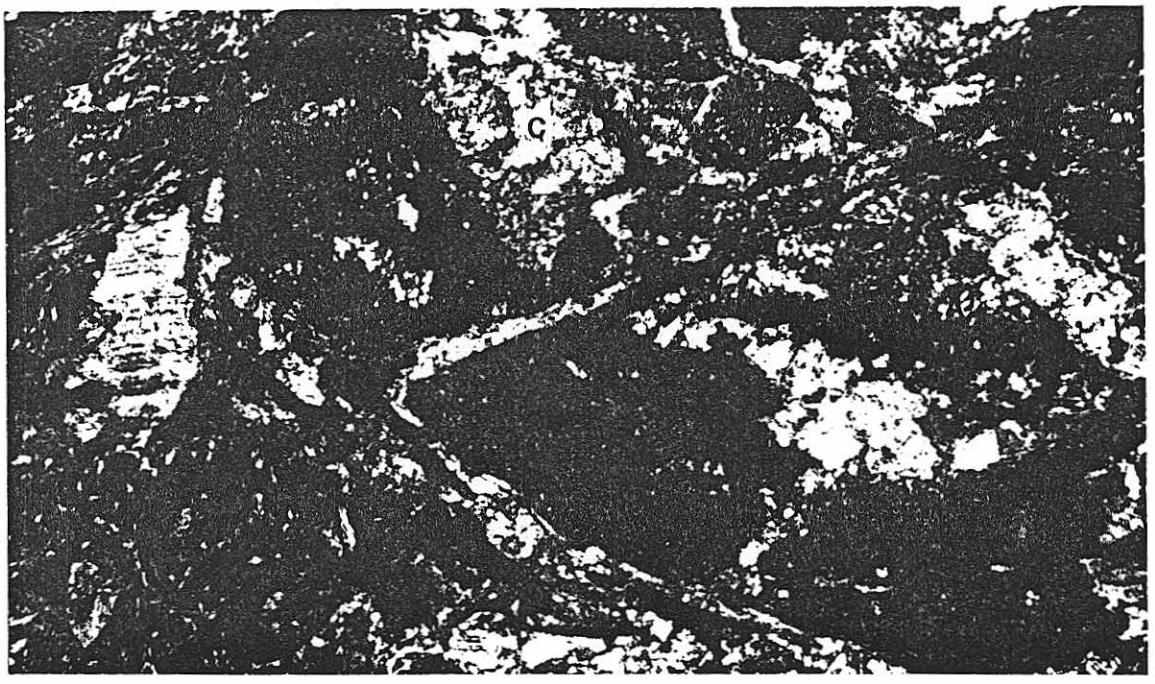

Fig. 7 γ-serpentine (chrysotile - A), alteration of talc (B), after carbonate (C). (3.125X).

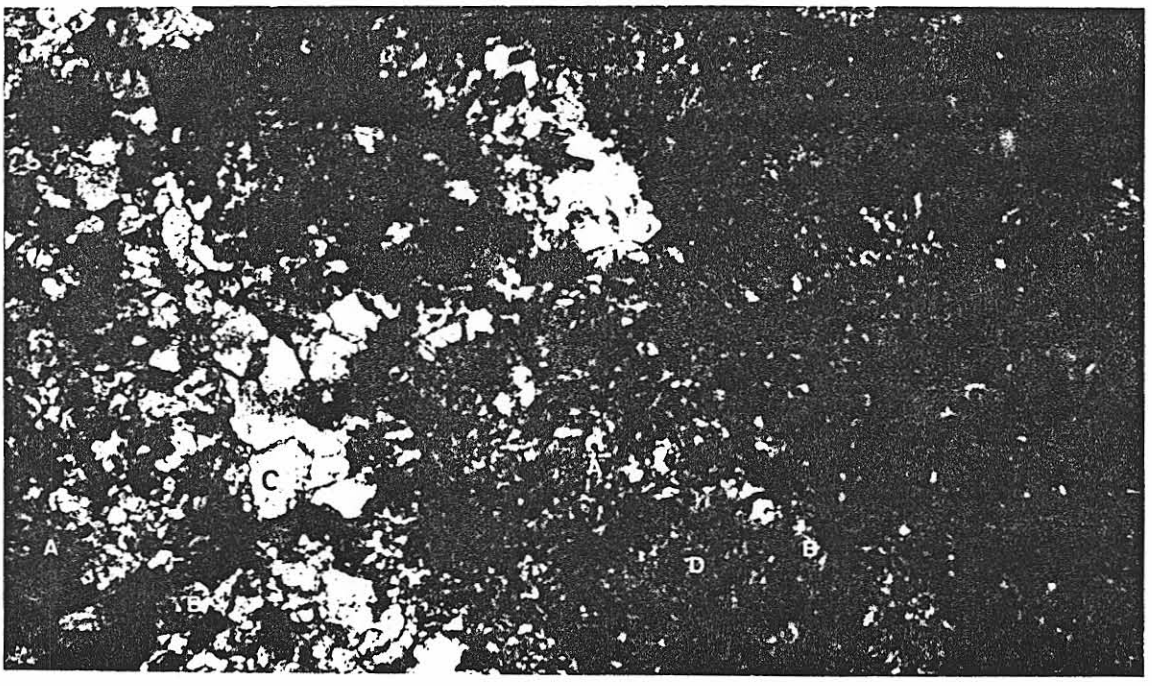

Fig. 8 Forsterite (A), diopside (B), calcite (C), assemblage. Tremolite (D) is also present, but is being replaced by diopside. (3.125X).

027

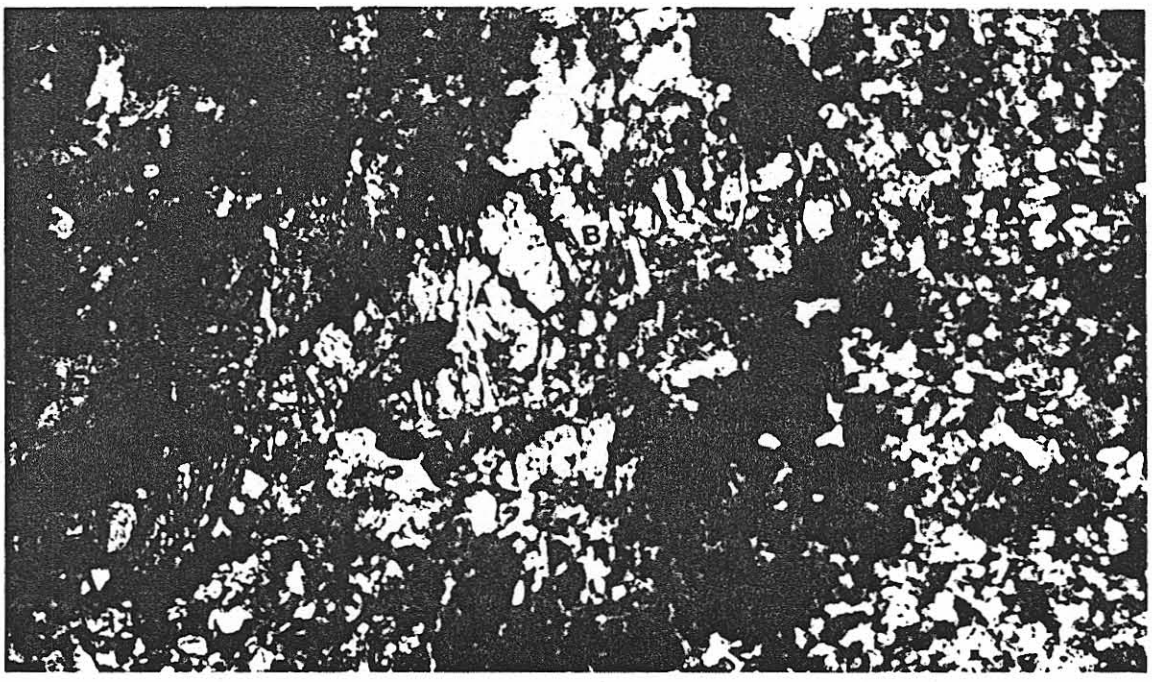

Fig. 9 Tremolite inclusions (A) in forsterite (B). Note serpentine alteration along fractures. (3.125X).

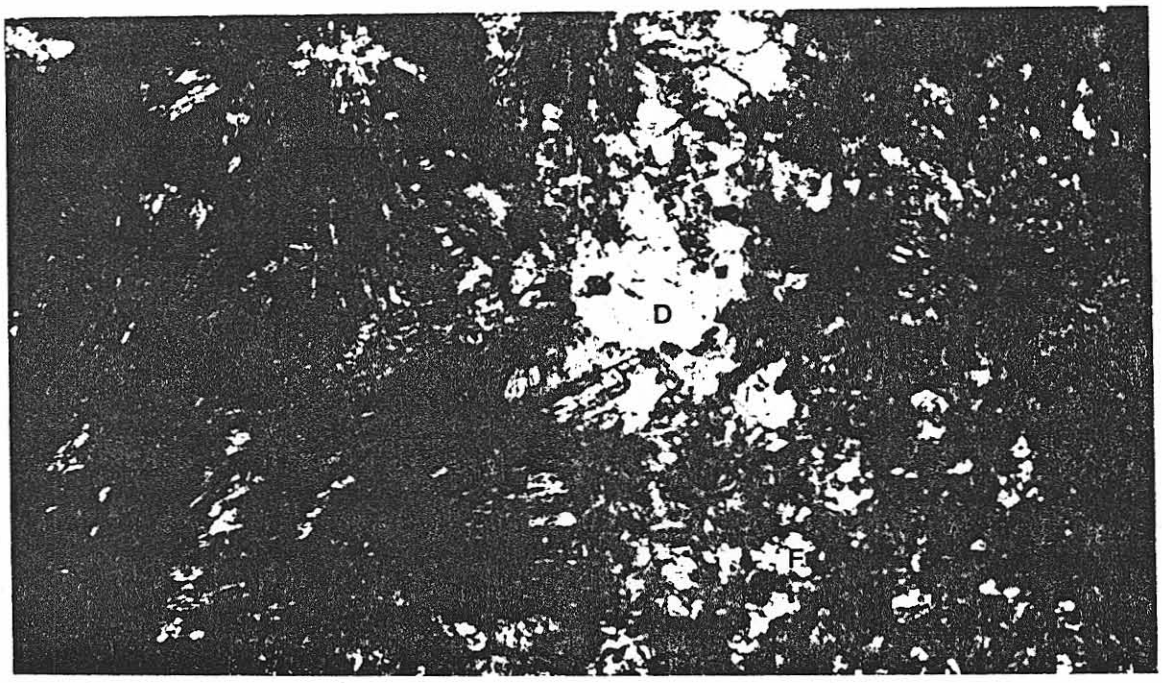

Fig. 10 Forsterite (A), diopside (B), tremolite (C), replacing carbonate (D). Magnetite needles (E) appear to be pseudomorphing the tremolite. Serpentine (F) alteration of forsterite and diopside can also be seen. (3.125X).

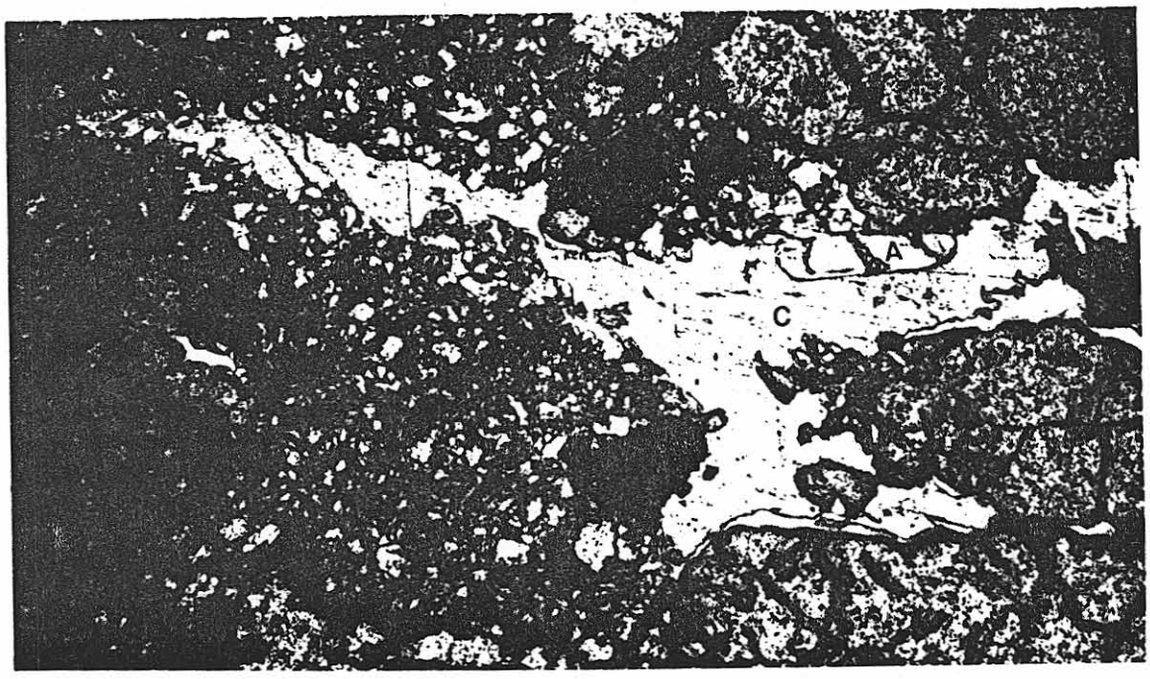

Fig.11 Diopside (A), andradite (B), calcite (C) skarn. Note large rectangular diopside crystal against andradite. (Plane polarised light. 3.125X).

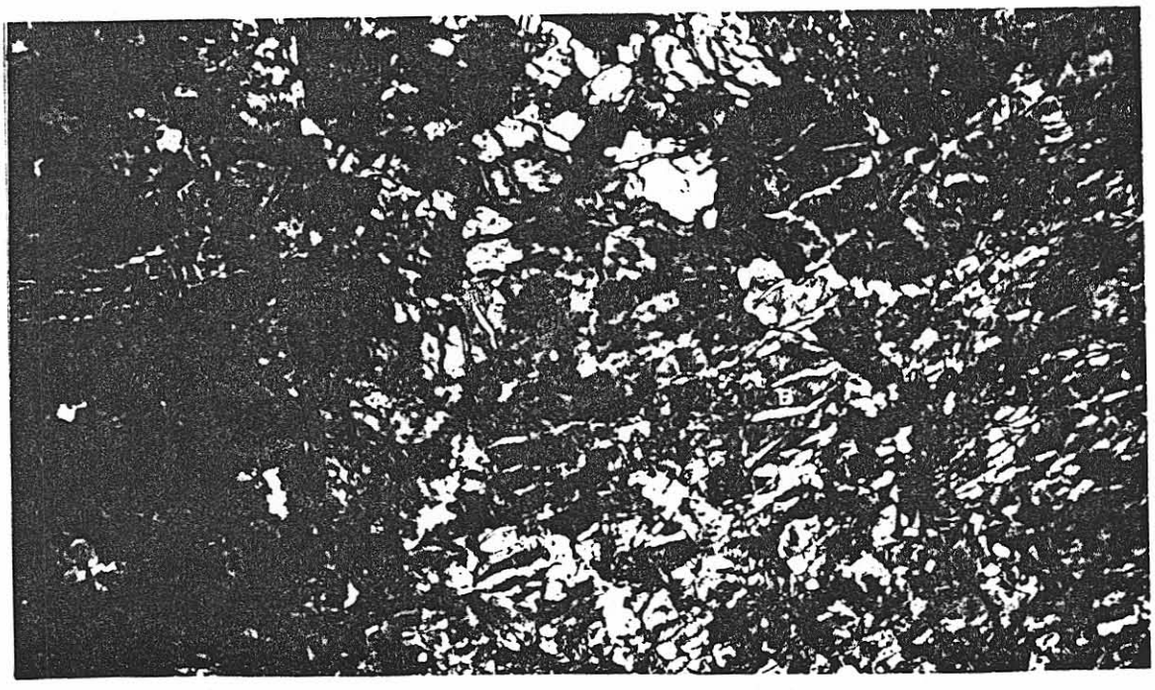

Fig. 12 Serpentine textures, (A) Bastite-serpentine pseudomorphs after magnesian silicates (B) Curtain textured serpentine which forms as a result of serpentine alteration along fractures in the original crystals. (3.125X).

029

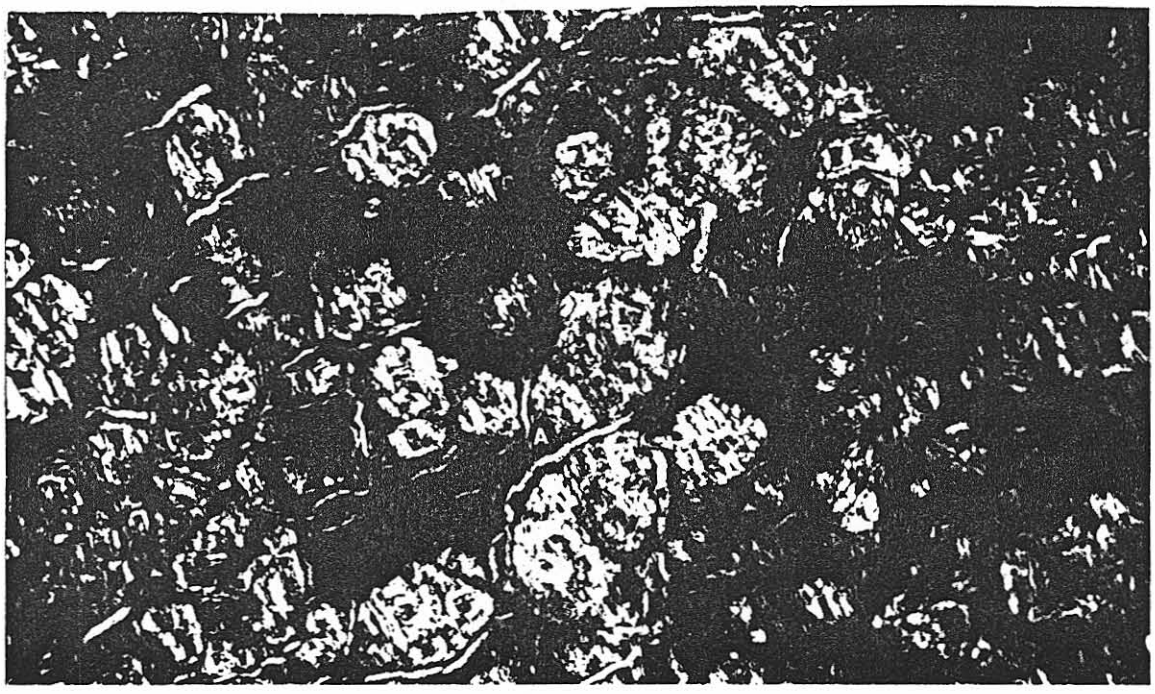

Fig. 13 Mesh texture after olivine γ-serpentine rims (A) surround cors of both α and γ-serpentine. (3.125X).

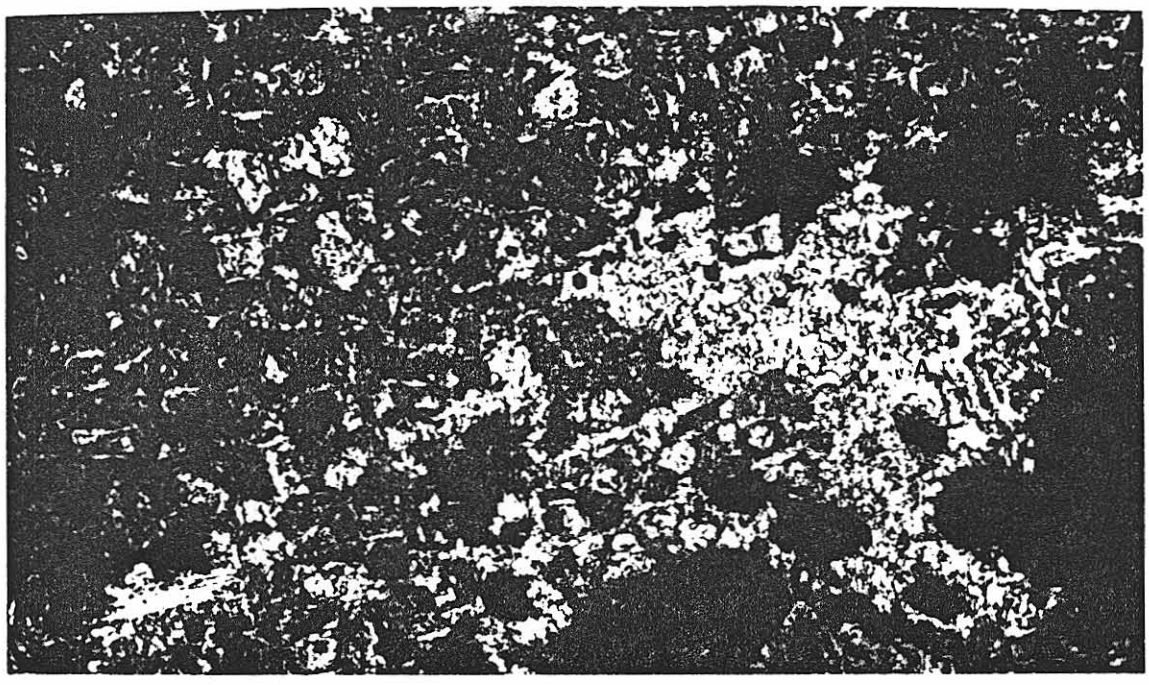

Fig. 14 Colourless interpenetrating γ-serpentine (A) surrounding opaque preferentially replaces mesh rims. Mesh centres (B) are largely altered to Fe-rich sheet silicate. (3.125X).

030

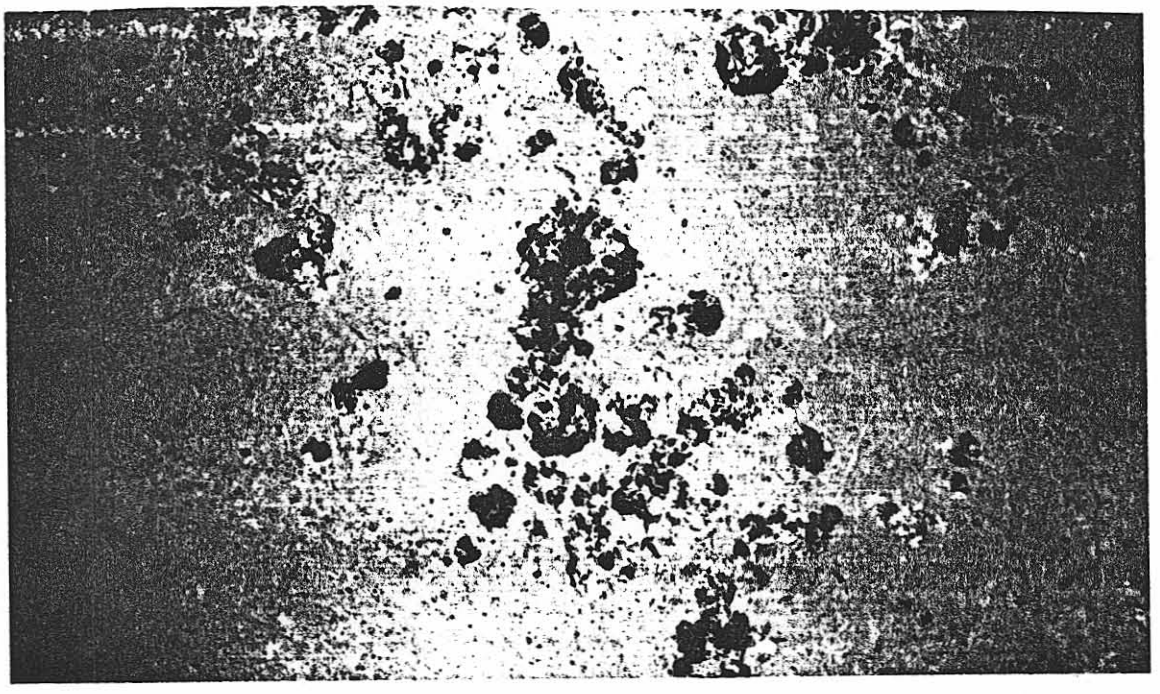

Fig. 15 Relict interlocking serpentine (A), surrounding relict opaques being replaced by interpenetrating γ-serpentine. (3.125X).

Fig. 16 Interpenetrating γ-serpentine (A) altering to amphibole (B) surrounded by fine grained interlocking and interpenetrating textured γ-serpentine (C). (3.125X).

031

Fig. 17 Talc (A) alteration interlocking and interpenetrating γ-serpentine(B) with relict bastite (C). (3.125X).

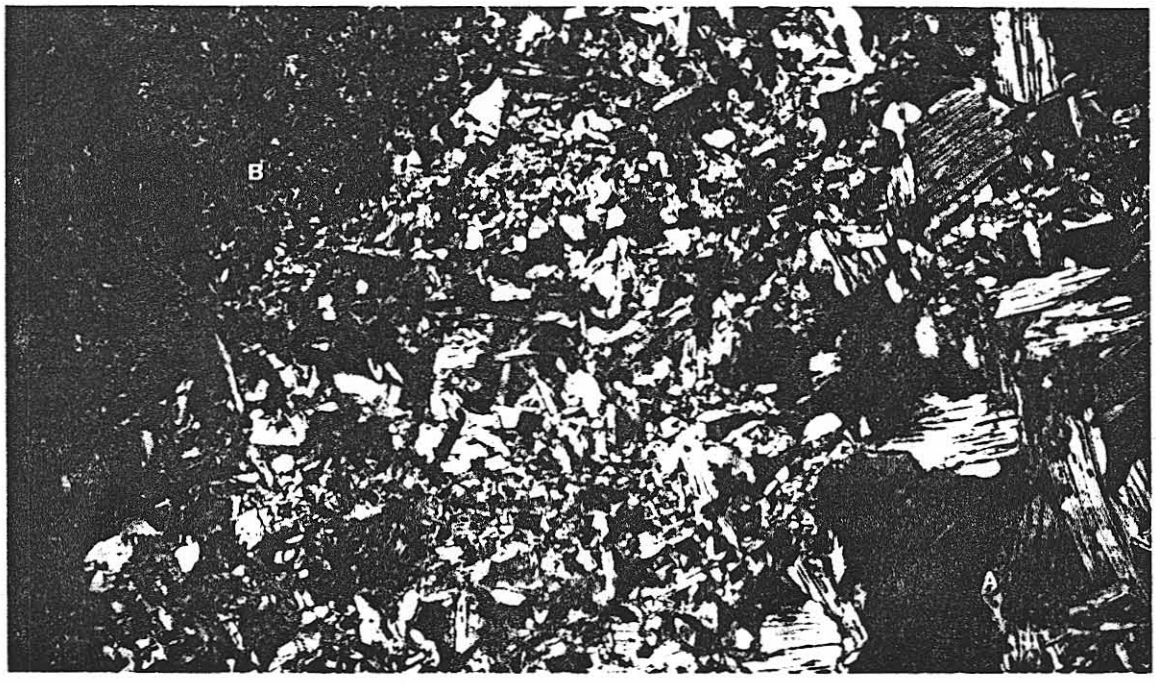

Fig. 18 Phlogopite (A) replacing diopside (B). Note sharp contact between diopside and phlogopite. (3.125X).

032

Fig. 19 Phlogopite alteration of curtain texture α and γ-serpentine. (3.125X).

Fig. 20 Olivine (A) in the initial stages of alteration along fractures to curtain textured serpentine with subsequent alteration to phlogopite (B). (3.125X).

033

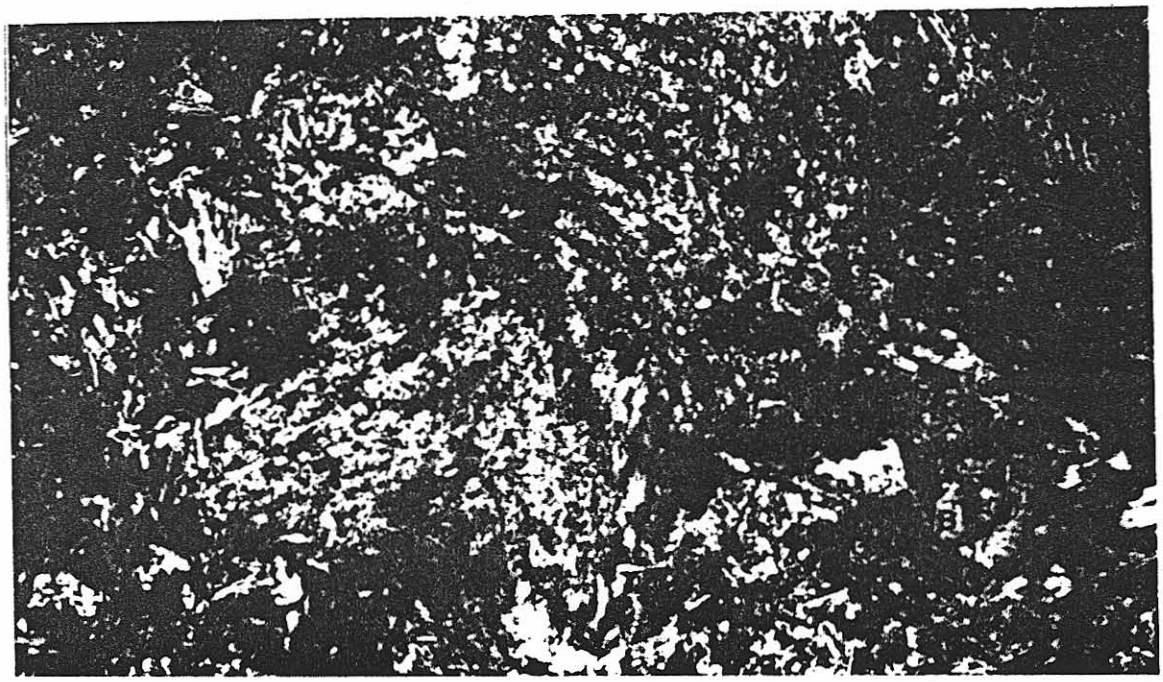

Fig.21 Late stage carbonate (A) replacement of diopside (B). (3.125X).

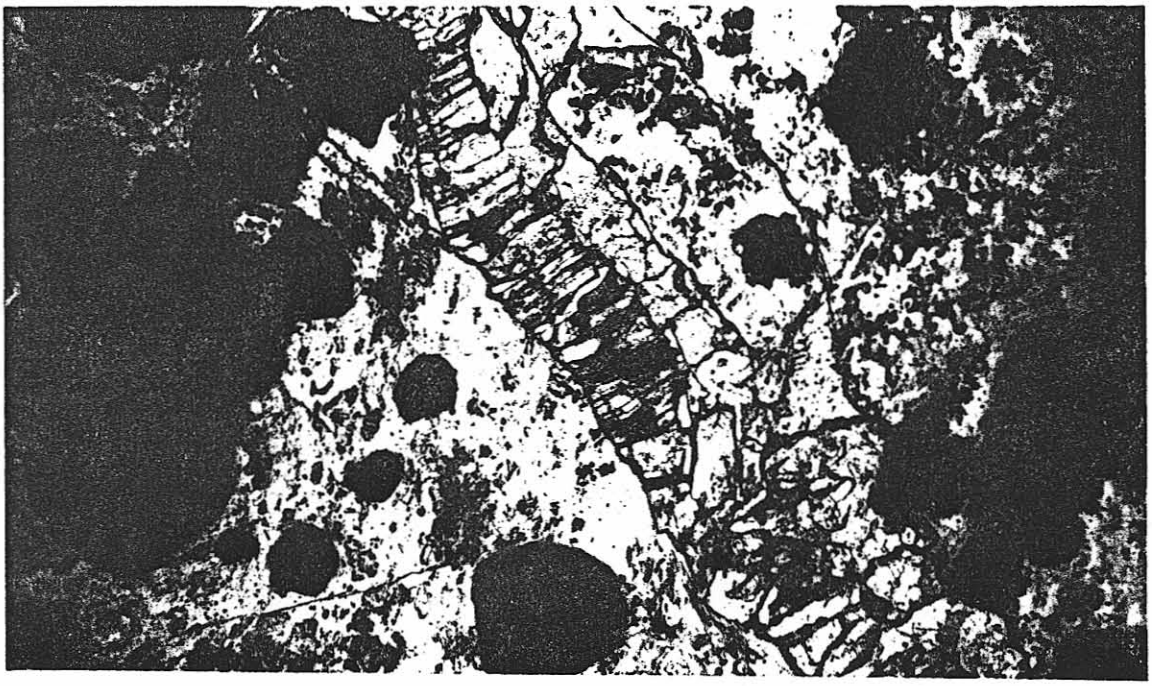

Fig. 22 Late stage calcite vein (A) through serpentine (B). (Plane polarised light 3.125X).

034

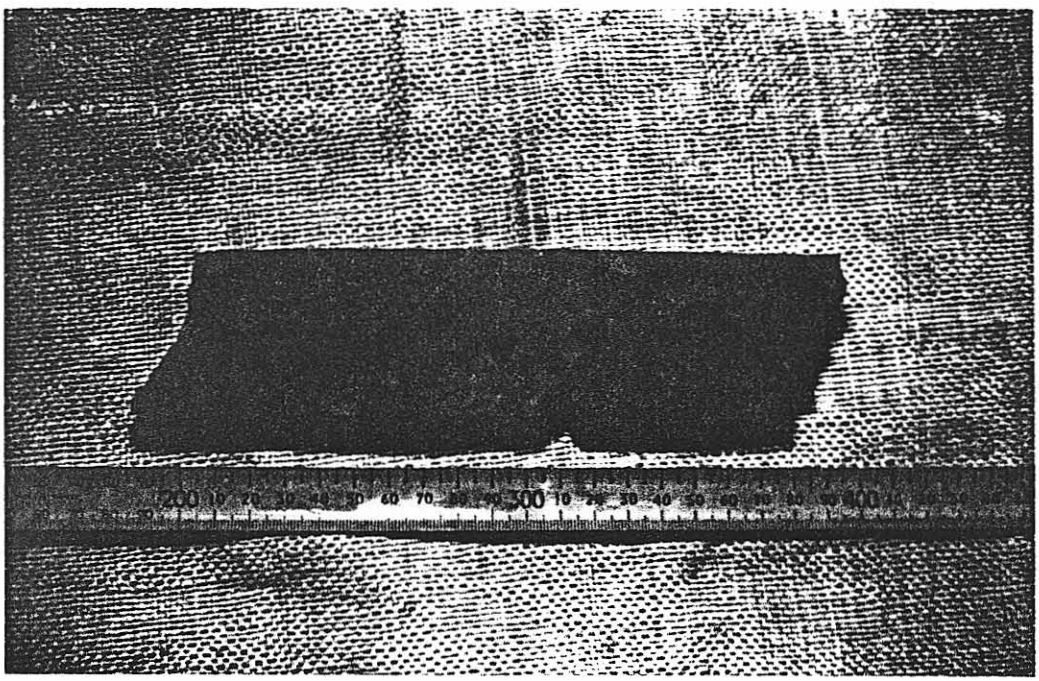

Fig.23 Late siderite (A) containing minor inclusions of pyrite in dolomite breccia (B).

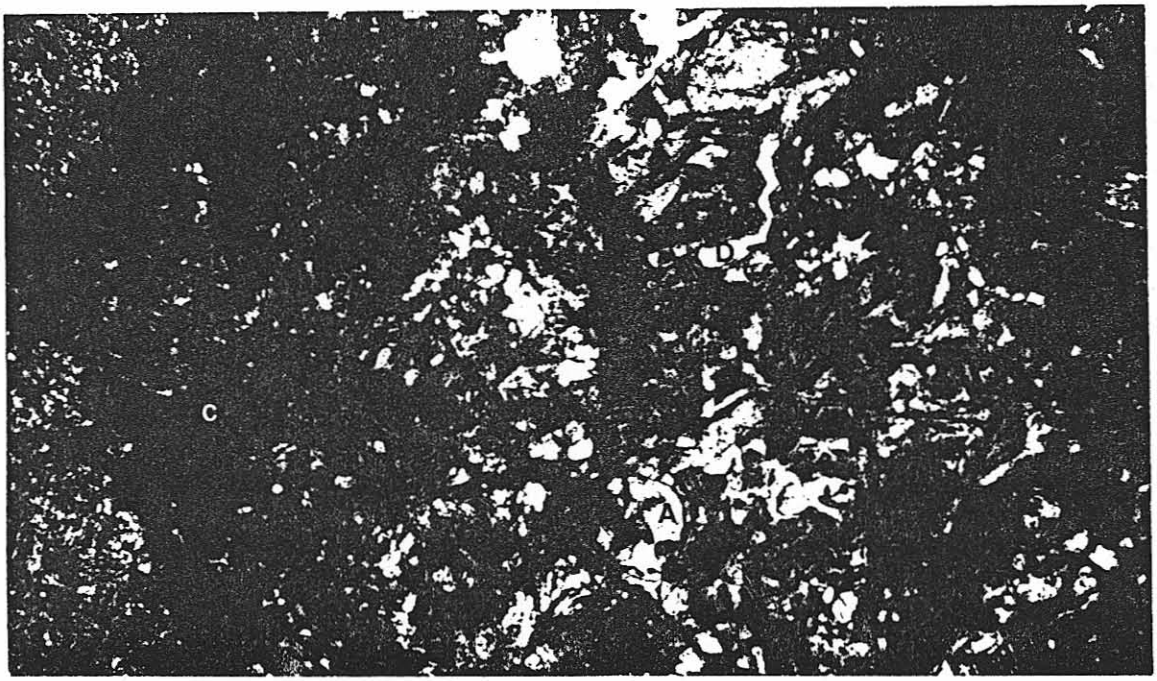

Fig.24 Vesuvianite (A) and serpentine (B) replacing diopside-wollastonite-calcite (C) with subsequent alteration of vesuvianite by epidote (D).

035

Fig.25 Epidote (A) alteration of grossular (B). The epidote is in turn replaced by Mg-chlorite (C). (3.125X).

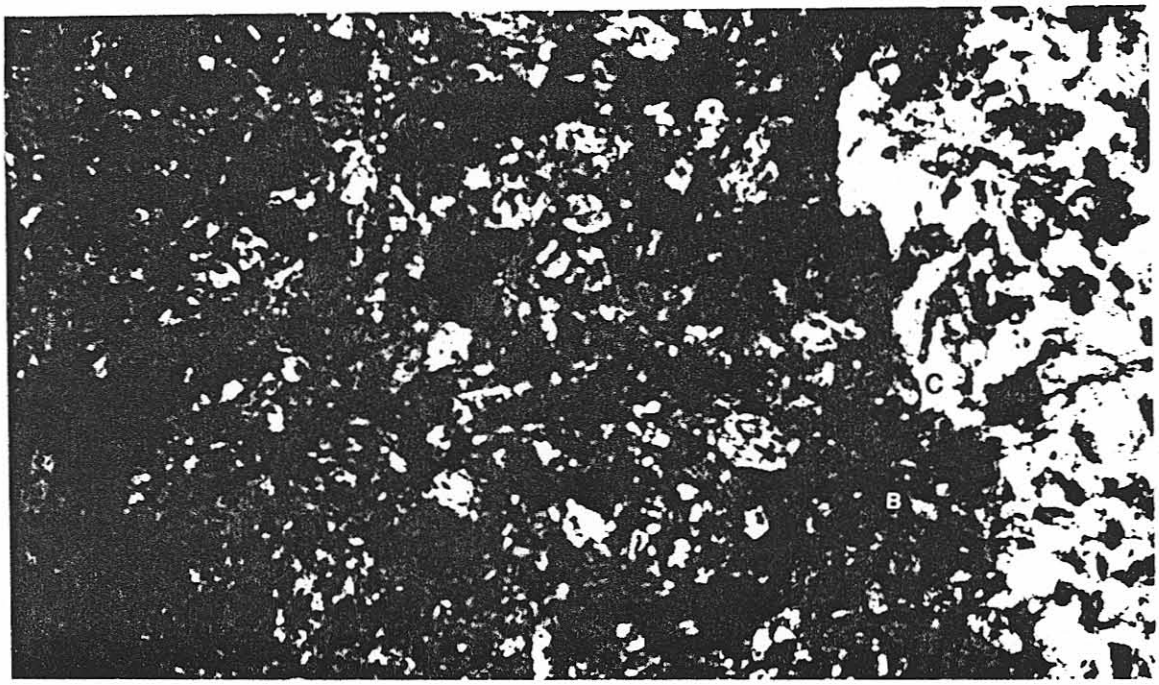

Fig.26 Epidote (A) alteration of diopside (B) wollastonite (C). (3.125X).

036

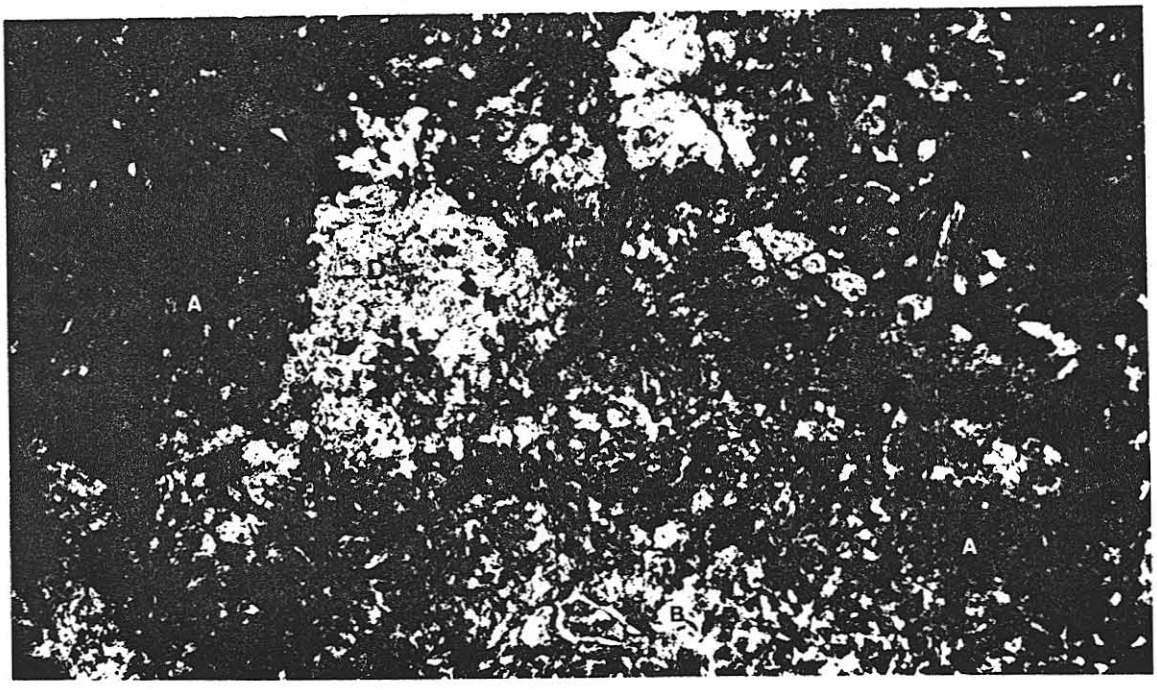

Fig.27 Ferrohastingsite (A) replacing diopside (B) with epidote (C) replacing garnet (D). (Plane polarised light 3.125X).

Fig.28 Epidote alteration of garnet showing typical replacement textures. Alteration begins along fractures in the garnet crystals. (3.125X).

037

The only alteration observed was in T.S. 13 - 69.8 where diopside alters to serpophite (isotropic serpentine).

4.3 Discussion of Alteration Sequence and Textures

Only those textures and assemblages crucial to the understanding of the alteration sequence are discussed in the following section. Important examples are illustrated with photomicrographs. The hydrous alteration affects both the contact metamorphic and ore skarn assemblages in a similar manner, (particularly the magnesium assemblages) and therefore is discussed in general terms to avoid repetition.

4.3.1 Alteration of Magnesian Skarn Assemblages

Subsequent to the formation of the various primary ore and metamorphic skarn assemblages from dolomitic marbles (Tables 1 and 2), the magnesium silicates underwent alteration. They may have experienced alteration during one or more stages (Table 2).

Stage II Alteration

The second stage of alteration after the formation of the calcium and magnesium silicates in stage one is dominated by serpentinisation. Serpentine alteration commences at the grain boundaries or along fractures within mineral grains (Figs.9 & 10). If the alteration proceeds to completion a number of distinctive textures result. Entire mineral grains may be replaced by serpentine which pseudomorphs the original material. This type of serpentine is called bastite. Curtain texture results when

038

alteration occurs along parallel or sub-parallel (T.S. 3 - 47.8) fractures which cut through the rock (Fig. 12). The serpentine in this example is both α and γ-serpentine (Appendix I).

Mesh-textured serpentine forms after olivine and may contain hourglass textures in their cores (Fig.13). Both α and γ-serpentine occur in mesh cores, whereas only γ-serpentine is present in mesh rims (T.S. 6 - 36.6).

Diopside alters to both bastite and curtain-textured serpentine. Bastite after amphibole cannot be distinguished from bastite pseudomorphing pyroxene if alteration is complete (Wicks and Whittaker 1977).

In Stage IIb of the alteration sequence the serpentine is recrystallised which destroys any evidence of the earlier formed textures. The recrystallised serpentine also has distinctive textures. These are interlocking and interpenetrating textures (Wicks and Whittaker 1977). The classification scheme in Appendix I suggests that the interpenetrating textured serpentine is most likely antigorite. Interlocking textured serpentine can be lizardite, chrysotile or antigorite. Figure 14 shows interpenetrating γ-serpentine which has largely replaced an earlier mesh texture. The centres of the mesh contain abundant magnetite surrounded by iron-rich sheet silicates (T.S. 2 - 26.4).

Interlocking textured serpentine is sometimes replaced by interpenetrating textured γ-serpentine (Fig.15; T.S. 2 - 96.6). This shows that the process of serpentinisation is more complex than just the two stages described earlier (Table 2).

029

Stage III

Alteration in Stage III may follow a number of different pathways. After the recrystallisation stage, the serpentine may be replaced by amphibole (Fig. 16 T.S. 8 - 57.6) and occasionally talc (Fig.17) or chlorite. Minor replacement of serpentine by chlorite occurs throughout the deposit.

Stage IV

Potassic alteration, which led to the formation of phlogopite, occurred in stage IV of the alteration sequence. The formation of phlogopite represents either a distinct and major change in the composition of the circulating metasomatic fluids, from solutions rich in silica, iron and sulphur to solutions rich in potassium and aluminium or a change in the P, T, fo_2, a_{SiO_2}, f_{CO_2}, etc. The phlogopite overprints all of the earlier formed assemblages to varying degrees. The alteration to phlogopite is most severe near the contact with the granite (see Map I). Fibrous magnetite appears to form concurrently with the potassic alteration, particularly near the contact.

The phlogopite alteration can overprint assemblages in any of the earlier stages of alteration. Fig.18 (T.S. 5.17.2) shows diopside being replaced by phlogopite, but serpentine and olivine may also be affected (Figs.19 & 20).

040

Stage V

The final stage in the alteration of the magnesium contact and ore skarn assemblages is late-stage overprinting by calcite and siderite. This stage is represented by the formation of veins or by the total replacement of earlier formed minerals by carbonate. Diopside (Fig.21, and phlogopite (T.S. 9 - 34.8) may be almost completely replaced by carbonate.

Most of the carbonate introduced in this stage occurs in veins. Calcite and siderite are the principal materials found in the veins (Figs.22 & 23). Siderite also occurs around the margins of massive magnetite and is usually surrounded by serpentine (T.S. 14 - 112:3).

5 SILICATE CHEMISTRY

Microprobe analyses of selected samples of the principal silicates from both the calcic and magnesian skarn are given in Appendix II. The analyses were made as part of the investigation into the tin mineralogy and for confirmation of optical mineral identification. Only general comparisons with published data have been made because of the limited number of analyses of each mineral. For the same reason no conclusions can be drawn about the variation in mineral composition between contact and distal assemblages.

041

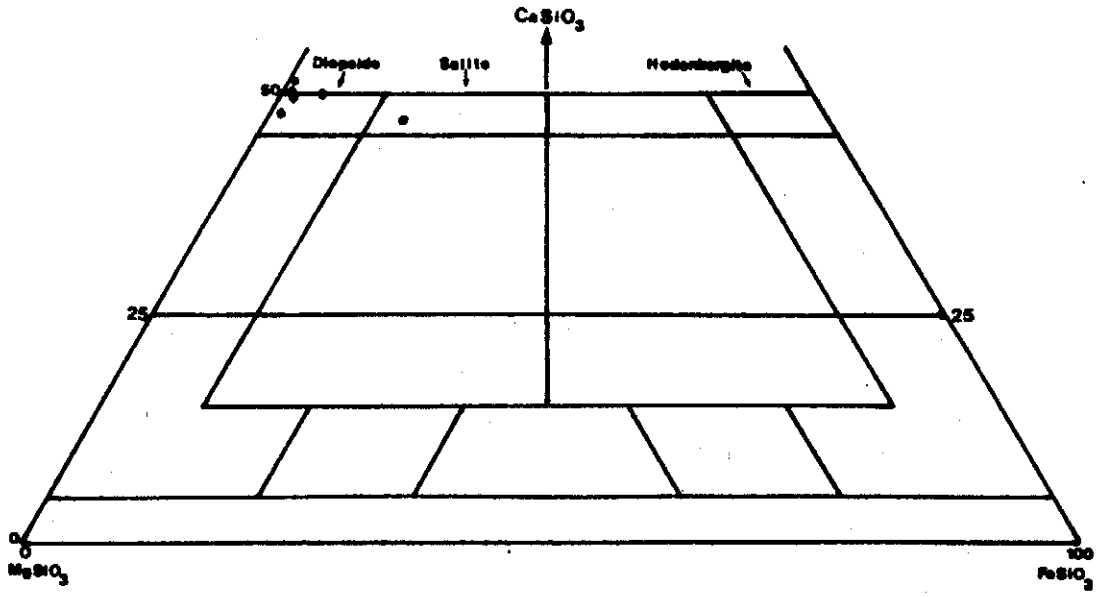

Fig.29 Nomenclature of clinopyroxene (after Poldvaart, A., & Hess, H.H., 1951, Journ. of Geol., Vol. 59 P.472).

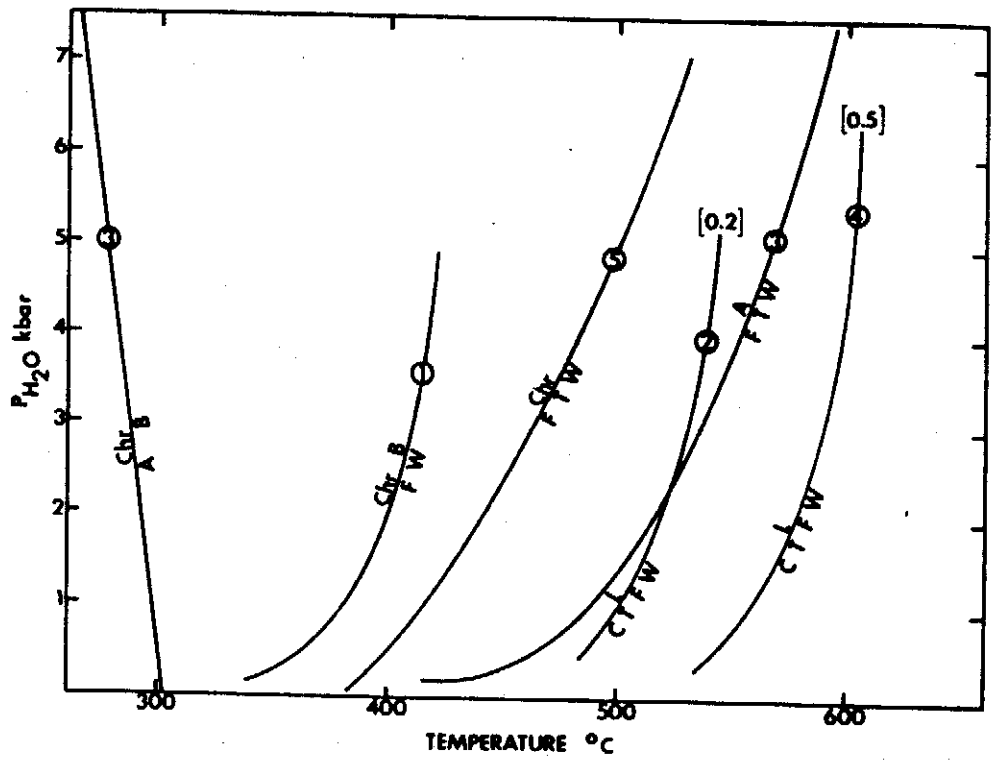

Fig.30 P-T diagram illustrating relative stabilities of chrysotile, lizardite and antigorite. Numbers in circles refer to source of data: (1) Johannes (1968), (2) Chernosky (1973a), (3) Evans et al. (1976), (4) Caruso, L.J., & Chernosky, J.V.J., The stability of lizardite, Can. Mineral. 17: 757-769, 1979.

042

Olivine

The results of analyses of olivines from Tenth Legion are given in Appendix III (analyses 1-3). Olivine Mg numbers (Mg/Mg+Fe) show these olivines to be forsteritic with compositions ranging from $Fo_{94.38}$-$Fo_{94.87}$. The forsterite content of olivines from Tenth Legion are higher than those found in most igneous rocks. The average composition of olivines from peridotites is Fo_{88}, whereas olivines from dunites have compositons as forsteritic as Fo_{92} (Deer et al. 1972). EDAX analysis of olivines from Tenth Legion using a Scanning Electron Microscope, returned negative results for Ni and Cr. This suggests that the Tenth Legion olivines have compositions different from those generally found in ultramafic rocks.

The Mg number of olivines from contact metamorphosed, impure dolomites at Boulder, Montana (Rice 1977), range from Fo95.8 to Fo99.9 which are similar in composition to those from Tenth Legion. The slightly higher rim contents of the olivines from Tenth Legion may be due to crystallisation during metasomatic alteration of the dolomite by siliceous iron-bearing fluids.

Pyroxene

Only one of the 8 pyroxenes analysed (analyses 4-9 and 21-22) plots outside of the diopside field in the pyroxene quadrilateral. The exception (analysis 5) plots in the salite field. Clinopyroxene with similar compositions are common in metamorphosed carbonates and skarns. No orthopyroxenes

043

(e.g. enstatite) were found at Tenth Legion, although they have been recorded in all the other dolomite skarns.

Amphibole

Amphiboles were analysed (analyses 12 & 13) from both the calcic and magnesian (analyses 10 & 11) skarns. A comparison of the data with published amphibole analyses (Deer et al. 1967), suggests that the dark green amphiboles from the calcic skarn are ferrohastingsite and the colourless amphiboles from the magnesian skarn are tremolite. Anthophyllite, edenite, tschermakite, and pargasite were not found at Tenth Legion, although they have been described from other dolomite replacement skarns and contact metamorphosed dolomite e.g. Boulder, Montana (Rice 1977).

Serpentine

Only two serpentines were analysed (analyses 14 & 15) and both of these came from the one sample. The totals for these analyses are about 5 wt% lower than normal values expected from serpentines and therefore they cannot be compared to other analyses. The low totals may be due to absorbed H_2O instability of serpentine when exposed to high accelerating currents in the electron microprobe.

Mica

A comparison of the mica analyses (analyses 16-19) with those in Deer et al. (1971) indicates that they are phlogopites.

044

This interpretation is also consistent with their optical properties. The two specimens analysed came from widely spaced localities (Map 1), but only differ slightly in their chemistry. The specimen from the nearest contact (D.D.H. 4-28) has slightly higher SiO_2, but is lower in Al_2O_3 than the more distal specimen (2-123.65). This variation should not be interpreted as being significant on the basis of only two analyses.

Chlorite

Three chlorites were analysed from the one sample (analyses 18 & 23-24). The chlorite in analysis 18 lies within the diabinite field of Deer et al. (1971:Fig.35) whereas the other two chlorites plot in the pycnochlorite field.

Plagioclase

The single plagioclase analysed (analysis 19) was found to be labradorite (An_{67}). This specimen came from a sample of calcic skarn containing diopside, wollastonite and garnet.

Garnet

Two specimens of grossular (analyses 20 & 27) and two specimens of andradite (analyses 25 & 26) were analysed. Both samples were from calcic skarn, but because of their higher iron content, the andradites must have come from ore skarn (see Section 4). Deer et al. (1972) suggests that grossular in calcsilicate rocks forms by the replacement of earlier formed wollastonite, and that andradite forms during Fe and SiO_2

045

metsomatism by the reaction;

$$3Ca\,CO_3 + Fe_2O_3 + 3SiO_2 \longrightarrow Ca_3\,Fe_2Si_3O_{12} + 3CO_2$$

calcite — andradite

Sphene

Sphenes (analyses 28-30) from the calcic skarn were probed in the hope that they would prove to be malayite (Sn - sphene). However, this was not the case and only one analysis (30) gave any indication of tin. (For further discussion of tin mineralogy see section 6).

Epidote

Three epidote analyses are given in Appendix III. These all came from a single sample of calcic skarn. The totals for the analyses are slightly low, but the compositions are still comparable with other published analyses of epidotes from metamorphic limestones (Deer et al. 1972).

6 ECONOMIC GEOLOGY

Compared with the minerals in the calcic and magnesian silicate skarn the metallic mineralogy is simple. The principal ore minerals and the alteration stages with which they are associated, are shown in Fig.35. It should be noted that the calcic skarn assemblages have only minor economic mineralisation and that the ore minerals shown in Fig.35 are confined almost

046

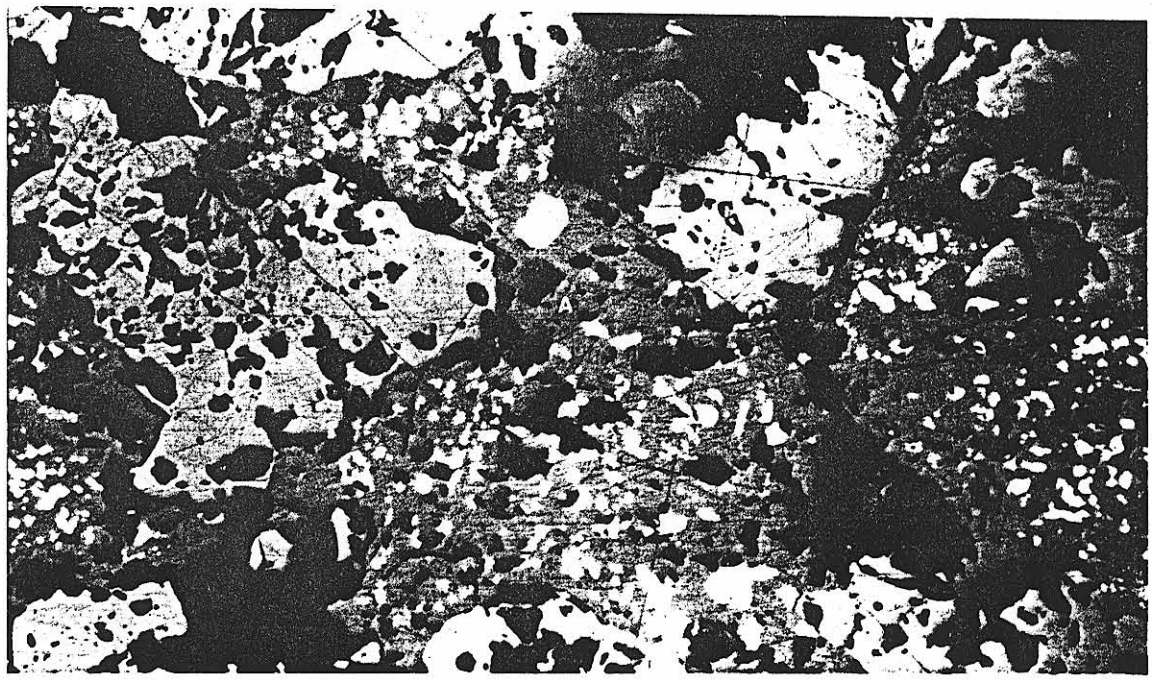

Fig.31 Sphalerite (A) replacing magnetite (B). The sphalerite contains inclusions of chalcopyrite (C).

Fig. 32 Pyrite replacing magnetite.

Scale

047

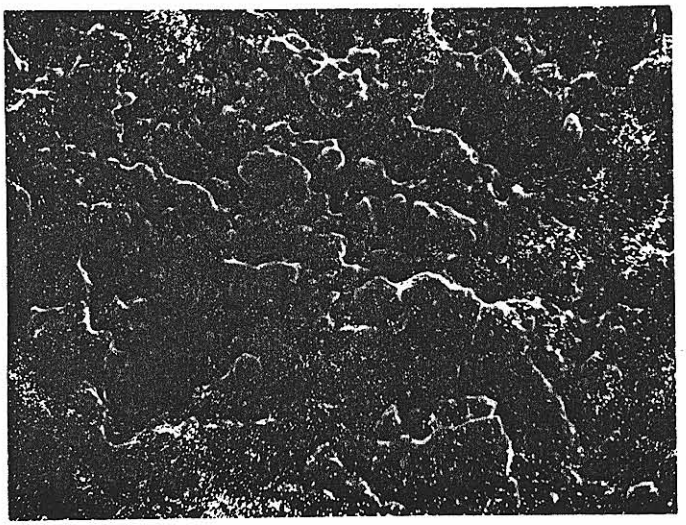

Fig.33 X-ray map with tin distribution and magnetite. Clusters of points indicate tin concentration. (1200X) At magnifications greater than this resolution is lost.

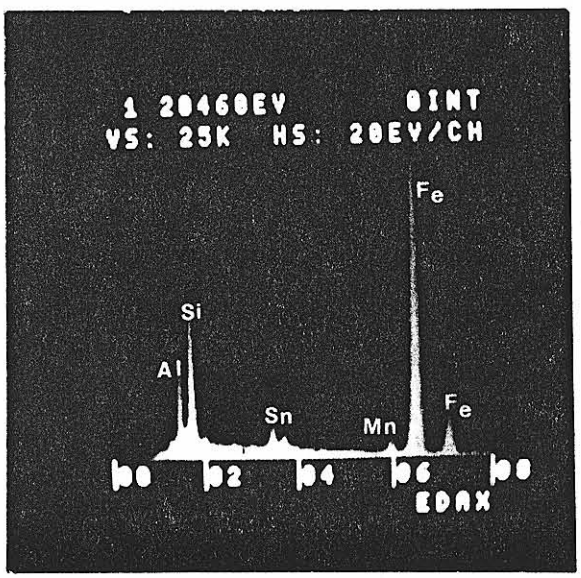

Fig.34 Results of EDAX analysis of magnetite showing peaks of major elements with tin showing up against background radiation.

Figure 35. ORE MINERALS IN RELATION TO THE MAGNESIUM ALTERATION SEQUENCE

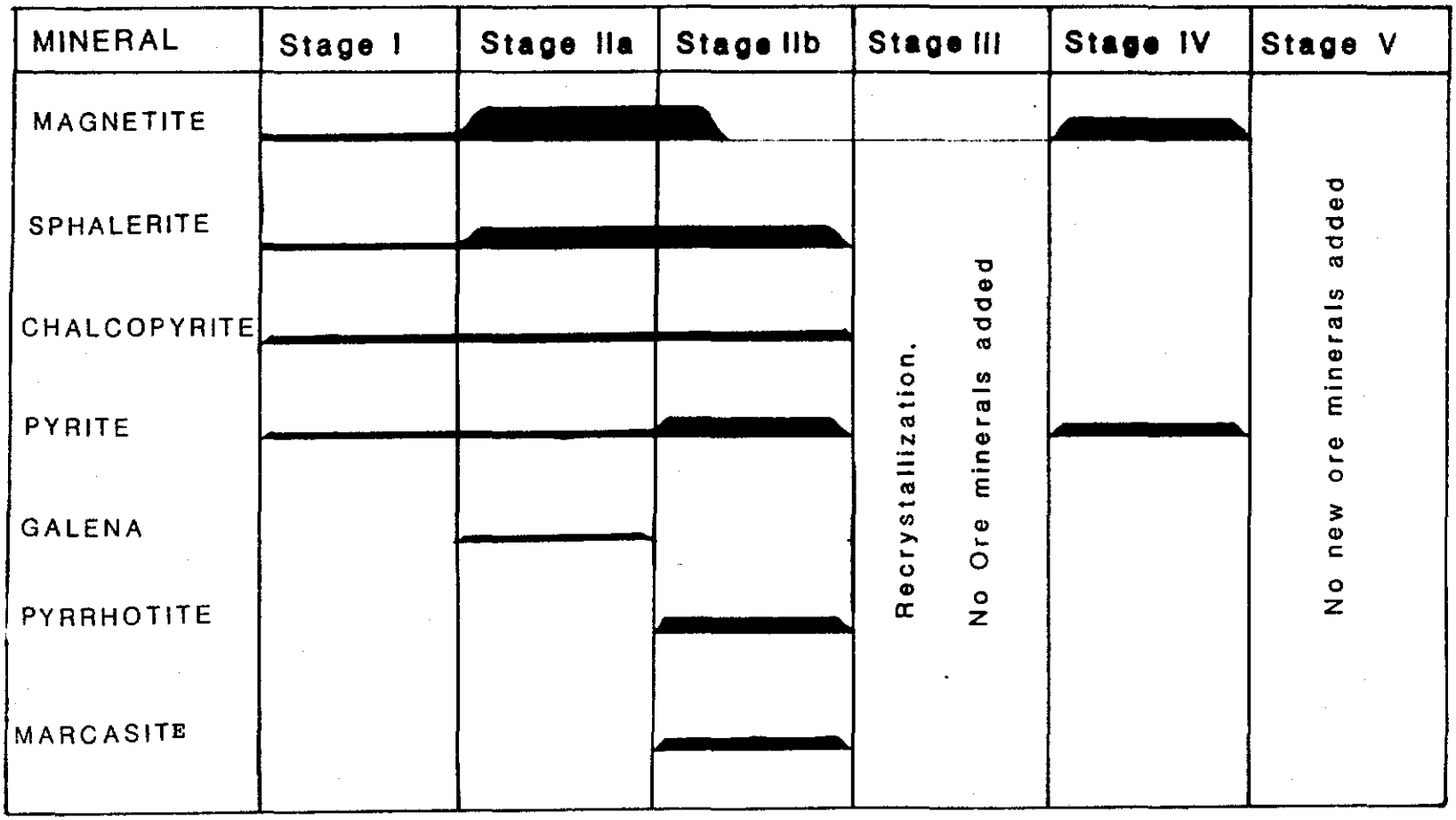

049

completely to the magnesian skarn. All assay values quoted are from C.R.A. drill core logs.

Iron

The principal iron mineral, magnetite, occurs in units up to 30 metres thick (the average thickness is less than 10 metres) and dessiminated throughout the silicates in the replacement skarn.

Iron sulphides are also present including pyrite, pyrrhotite and marcasite. The latter two minerals are only minor phases in the deposit.

Zinc

Sphalerite occurs in massive units up to a metre thick with average values of 1%. One drill hole (DDH 1) however, intersected a unit 25 metres thick that returned assays averaging 1.16% Zn. The unit also contained diopside, tremolite, epidote, magnetite and serpentine skarn horizons. In another exceptional example 1 metre of 11% Zn was intersected.

Copper

The only copper mineral found at Tenth Legion was chalcopyrite which usually occurred as inclusions in sphalerite (Fig.31) and as infillings along fractures in pyrite. Average assays were less than 1%.

050

Tin

In drill hole 1 (Fig.2 & Map 1) tin assays returned values of between 0.3 and 3.3% Sn in massive magnetite over an interval of 3 metres. Tin values ranging from 0.1 to approximately +1% were encountered in drill hole 9 over two intervals of massive magnetite 6.7 and 7.4 metres thick.

An extensive investigation of all three occurrences using ore mineragraphic techniques and SEM failed to produce any conclusive results concerning the nature of the tin complexes. The results of the X-ray mapping by EDAX and SEM are shown in Figs. 33-34. From Fig.33 it can be seen that the Sn is not randomly distributed, but occurs in clusters in magnetite. The resolution, at magnifications greater than 800X, was too poor to allow a more thorough investigation of the nature of the tin complexes.

Aleksandrov (1973) suggested that although magnetite may contain up to 0.45% Sn in the lattice, most Sn is located in crystal lattice defects. Tin may also substitute for Fe^{3+} in amphibole, garnet, epidote or sphene (Mulligan and Tambor, 1968, but as shown in the microprobe results (Appendix III) this does not appear to be the case at Tenth Legion. The average background values from core logs range from 50-100 ppm in the skarn assemblages.

051

Gold - Silver - Lead - Tungsten

These four metals only occur in trace amounts at Tenth Legion. Ore minerals containing these elements were not found in the skarn. One metre of core from DDH 6 assayed at 1.34g/tonne gold. Lead values are mostly less than 0.2% but Ag reached a maximum of 10.6gm/tonne. Maximum W values are in the order of 400 ppm, but the average would be much less than this.

Textures

Fig.35 shows that magnetite is the principal ore mineral associated with the initial stages of alteration. However, pyrite, pyrrhotite and even sphalerite may occur in small quantities in massive marbles devoid of any apparent silicate alteration (T.S. 2-81.9 and 7-23). The bulk of the magnetite appears to be introduced during early serpentinisation (stage IIa) prior to recrystallisation of the serpentine (stage IIb). The magnetite which often has ilmenite exsolution lamellae is subsequently replaced by sulphides, particularly pyrite (Fig.32; T.S. 9-67.2) and sphalerite (Fig.31; T.S. 8-53). It is possible that the replacement of magnetite by the sulphides occurs during the recrystallisation stage (IIb), but conclusive evidence for this is lacking.

The pyrite may alter to either pyrrhotite (T.S. 4-91.4) or marcasite (T.S. 2-81.75). Sphalerite nearly always contains chalcopyrite inclusions.

Fibrous magnetite is found during the potassic alteration stage and is subsequently replaced by pyrite which is in turn replaced by pyrrhotite. Textural evidence (Fig.15) suggests that fibrous magnetite forms as a pseudomorph after amphibole (Fig.15). The formation of ore mineral assemblages culminated with the fibrous magnetite and its subsequent alteration to pyrite.

7 DISCUSSION

7.1 Tenth Legion Deposit - Skarn or Altered Ultrabasic?

As described previously, earlier workers on the metallic ore deposits of the Zeehan district (Hughes 1958, Solomon 1962, Blissett 1962) regarded Tenth Legion as having formed from the alteration of ultramafic or basic igneous rocks. They based their interpretation on the similarities between the massive magnetite and serpentine at Tenth Legion with the nearby Savage River iron ore deposits and the proximity of Tenth Legion to gabbroic rocks. This study does not support the interpretation advanced by these workers.

The evidence against Tenth Legion being an altered ultramafic is as follows:

053

1. The pyroxene, olivine, serpentine and magnetite assemblages which are suggestive of an ultramafic origin are interbedded with hornfels, dolomitic marble horizons and calcic silicate skarn containing andradite and grossular garnet.

2. EDAX analyses returned negative results from Ni and Cr in both the magnetite and the olivines, but showed Sn to be present in the magnetite (Figs. 33 & 34).

3. The olivines have compositions that are more forsteritic (Appendix III analyses 1-3) than olivines in most ultramafic rocks.

4. Large scale serpentine and carbonate alteration appears to be absent from the adjacent gabbro (Map 1). This alteration might be expected if the magnetite was associated with this unit.

7.2 Conditions of Formation

Only general conclusions concerning the approximate conditions of formation of the Tenth Legion skarn can be made since detailed fluid inclusion data is not available. A comparison of the stable contact assemblages at Tenth Legion with those given by Turner (1981) suggests that during contact metamorphism conditions ranged from albite-epidote-hornfels facies, represented by the assemblages talc-calcite-dolomite, to pyroxene hornfels facies (diopside-grossular-plagioclase and diopside-wollastonite-vesuvianite). Thus the lowest temperature must have been about 250°C with an upper limit of approximately

700°C. The forsterite assemblages are regarded as having formed at metamorphic grades equivalent to hornblende hornfels facies.

The approximate conditions that prevailed during stage II can be ascertained from Figure 3 which shows the experimentally determined univariant curves for the system MgO - SiO_2 - H_2O. A maximum temperature of 500°C can be placed on stage IIa by the serpentine (lizardite/chrysotile) - forsterite-talc univariant curve. The absence of brucite from Tenth Legion suggests that minimum temperatures were above 350°C during stage IIa (assuming $a_{H_2O} = 1$). During stage IIb temperatures were in excess of 400-450°C up to 550°C. Talc alteration of serpentine must have occurred at temperatures above the antigorite stability field i.e. > 550°C. No data is available on tremolite alteration of serpentine, but it probably also took place above 550°C. The conditions that prevailed during the potassic alteration stage (stage V) are unknown. Late stage chrysotile veins represent retrograde metamorphism at temperatures less than 450°C.

7.3 Formational History

The earliest recognisable assemblages are those containing talc, forsterite, diopside and tremolite in the magnesian skarn and wollastonite, diopside, grossular, and andradite in the calcic skarn. The contact metamorphic assemblages are overprinted by the ore skarn assemblages. It is assumed that skarn formation is related to the intrusion of the Heemskirk Granite, but direct evidence for this is lacking.

055

The primary ore skarn assemblages were formed by the reaction of Fe, SiO_2 and S-bearing fluids with carbonates. This resulted in the crystallisation of talc, forsterite, diopside and tremolite assemblages in the magnesian skarn. In the calcic skarn the Fe was incorporated into silicates e.g. andalusite.

In stage IIa the earlier formed magnesian silicates were hydrated to lizardite and chrysotile. This represents retrograde metamorphism of the contact and ore skarn assemblages. During stage IIb the lizardites and chrysolite were recrystallised to antigonite. The bulk of the metallic mineralisation is believed to have occurred at the same time as serpentinisation. The repeated occurrence of massive sulphides and magnetite with serpentine alteration suggests that they formed contemporaneously. It is not possible with the present data to determine which part of stage II was accompanied by the metallic mineralisation. Epidote alteration of calcic contact metamorphic skarn assemblages occurs in either stage I or during stage II alteration of magnesian skarn assemblages. The formation of epidote from grossular, vesuvianite, wollastonite and diopside requires Fe which is assumed to be introduced during these stages.

In stage III, the alteration consisted of the recrystallisation of the earlier formed serpentine to tremolite, talc or chlorite. Stage III occurred at higher temperatures than stage IIa.

Potassic alteration occurred during stage IV and is represented by the widespread occurrence of phlogopite which

overprints all earlier assemblages. The phlogopite alteration is most intense near the contact, but it is not known if it is related to the albitisation of the granite. Fibrous magnetite was formed during the potassic alteration stage near the granite contact and was subsequently replaced by pyrite.

The final stage in the alteration sequence is represented by late calcite and siderite veins along fractures in the skarn rocks. Calcite veins occur most commonly in the serpentine assemblages. The chrysotile veins which cut across the massive serpentine marble units are thought to be part of this retrograde event.

7.4 Concluding Statement

Contact metamorphic skarn is produced by reaction between carbonate and hornfels during contact metamorphism. This produced magnesian and calc silicate skarn, which are distinct from the ore skarn. The latter is produced during metasomatism by SiO_2,S and Fe-bearing fluids. Separation of contact metamorphic and ore skarns may be somewhat artificial as both types of skarn are formed by processes associated with a single event. There is some overlap between the two and the processes involved in the formation of one could be involved in the formation of the other. Later alteration may affect both types of skarn.

The phlogopite alteration is probably equivalent to the biotite and K - Al acid leaching stages described from Lost

057

River (Dobson 1982). Where serpentine has been described from other deposits e.g. Kitelya (Materikov 1977), it is regarded as being part of the post-ore retrograde sequence. However, at Tenth Legion, serpentinisation is believed to accompany metallic mineralization. Tenth Legion is not economic, unlike similar deposits in the Soviet Union. Potential exists for similar and perhaps economic deposits to occur in north-west Tasmania. The absence of extensive borate and fluorine minerals might help to explain the lack of economic tin mineralization, particularly if tin is transported as borate and fluorine complexes.

058

REFERENCES

Aleksandrov, S.M., 1974, Geochemistry of B-Sn mineralisation in the magnesian skarns of Eastern Chukota. Geochemistry International, Vol 11, No.532-539.

Aleksandrov, S.M., 1975, Geochemical aspects of B-Sn ore formation in Alaskan deposits. Geochemistry International Vol 12, 2 pp. 139-150.

Blissett, 1962, Geological survey explanatory report - One mile geological map, series K55-50- Zeehan, Tasmanian Department of Mines.

Both, R.A., & Williams, K.I., 1968, Mineralogical zoning in the Pb-Zn ores of the Zeehan Field, Tasmania. Part I: Introduction and review. 15 (1) pp. 121-137. J. Geol. Soc. Aust.

Mineralogical zoning in the Pb-Zn ores of the Zeehan Field Tasmania, Part II: Panagenetic and zonal relationships. J. Geol. Soc. Aust. 15 (2) pp. 217-243.

Brooks, C., 1966, The Rb-Sr ages of some Tasmanian igneous rocks, J. Geol. Soc. Aust. 13 (2): pp.457-469.

Brooks, C., & Compston, W., 1965, The age and initial Sr^{87}/Sr^{86} of the Heemskirk Granite Western Tasmania, J. Geophys. Research, Vol. 20, No. 4, pp. 6249-6262.

Burt, D.M., 1977, Mineralogy and petrology of skarn deposits, Rendiconti, Societa Italiana di Mineralogia e Petrologia, 33 (2) 859-873.

Corbett, K.D., & Brown, A.V., 1976, Geol. of Queenstown Sheet.

Dobson, D.C., 1982, Geology and alteration of the Lost River tin-tungsten-fluorine deposit Alaska, Economic Geology, Vol. 774: pp.1033-1052.

Einaudi, Meinart & Newberry, 1981, Skarn Deposits, Economic Geology, 75th volume, Vol. 76, pp.317-391.

Einaudi, M.T., & Burt, D.M., 1982, A special issue devoted to skarn deposits. Introduction-terminology classification and composition of skarn deposits, Economic Geology, Vol. 77 Part 4, 745-754.

Hall, G., & Solomon, M., 1962, Metallic mineral deposits, J. Geol. Soc. Aust., 9, pp.285-309.

Heier, K.S., & Brooks, C., 1966, Geochemistry and the genesis of the Heemskirk granite, West Tasmania. Geochemica e Cosmochimica. ACTA Vol. 30, pp.633-643.

Hughes, T.D., 1958, Magnetite deposits at Tenth Legion, Constock district. Tas. Dept. Mines, Technical Report No.3, pp.42-54.

Kwak, T.A.P., & Askins, P.W., 1981, The nomenclature of carbonate replacement deposits, with emphasis on Sn-F(-Be-Zn) 'wrigglite' skarns, J. Geol. Soc. Aust., 28, 123-136.

Materikov, M.P., 1977, Deposits of tin, Smirnov VI. Ed. Ore deposits of the Soviet Union, Vol. III Pitman.

Mulligan, R., & Jambor, J.L., Tin-bearing silicates from skarn in the Cassiar district, Northern British Columbia, Canadian Mineralogist, Vol. 9 (3) pp.358-370.

Rice, J.M., 1977, Contact metamorphism of impure dolomitic limestone in the boulder aureole, Montana. Contrib. Mineral & Petrol. 59, pp.237-259.

Raheim, A., & Compston, W., 1977, Correlations between metamorphic event and Rb-Sr ages in metosediments and from Western Tasmania. Lithos. 10, pp.271-289.

Sainsbury, C.L., 1968, Geology of the Lost River mine area, Alaska. U.S. Geol. Survey Bull. 1129, p.80.

Shabynin, L.I., 1971, Deposition of magnetite ores, magmatic stage, in the magnesiaskarnal ore-bearing foundation. Internat. Geol. Rev. 13 (12) 1798-1805.

Solomon, M., 1981, An introduction to the geology and metallic ore deposits of Tasmania, Economic Geology, Vol. 76, pp.194-208.

Turner, F.J., 1981, Metamorphic petrology, Hemisphere Pub. Corp.

Twelvetrees, W.H., 1901, Report on the mineral districts of Zeehan and neighbourhood. Rep. Secr. Mines. Tasm. (1900-1901), pp.5-108.

060

Waller, G.A., 1903, Report on the iron-zinc-lead ore deposits of the Comstock district, Rep. Secr. Mines.

Ward, L.K., 1912, An investigation of the relationship between the ore-bodies of the Heemskirk-Comstock-Zeehand region and the associated igneous rocks. Rep. Australas. Ass. Advmt. Sci., 13, pp.148-164.

Waterhouse, L.L., 1916, The South Heemskirk tin field, Geol. Survey Tasmn. Bull. 21.

Wicks, F.J., & Whittaker, E.J.W., 1977, Serpentine textures and serpentinization. Can. Mineral. pp.459-488.

Woolnough, W.G., 1939, Report on the examination of iron ore deposits of the Five Mile district Zeehan. Rep. Dep. Min. Tasm.

061

APPENDIX I

Table 4. SERPENTINE IDENTIFICATION CHART FOR THIN SECTIONS

Texture	Optical Character	Mineralogy
PSEUDOMORPHIC TEXTURES*		
mesh rim	α	- lizardite**= brucite
	γ	- lizardite, antigorite or chrysotile
Mesh centre	α γ + is	- commonly lizardite + brucite, rarely - antigorite or chrysotile = brucite
hourglass	α	- lizardite = brucite
	γ	- antigorite or chrysotile
clinopyroxene-bastite	α	- lizardite
	γ	- lizardite
amphibole-bastite	α	- lizardite, rarely with brucite
	γ	- lizardite, rarely with brucite
phlogopite-bastite	α	- not found
	γ	- lizardite, rarely with brucite
talc-bastite	α	- not found
	γ	- lizardite, rarely with brucite
chlorite-bastite	α	- not found
	γ	- antigorite or lizardite
NON-PSEUDOMORPHIC TEXTURES*		
interlocking	α	- lizardite IT or multilayer polytype possibly with some chrysotile
	γ	- chrysotile and/or antigorite
interpenetrating	α	- not found
	γ	commonly antigorite, less commonly - chrysotile and/or lizardite
VEIN SERPENTINE*		
non-asbestos (fracture filling)	α	- lizardite IT or multilayer polytypes chrysotile and/or lizardite or ♦
	γ	- antigorite = brucite chrysotile and/or lizardite = brucite

is - isotropic

* Brucite can very rarely be identified with the microscope in pseudomorphic textures and some non-asbestiform veins, so the possibility of its presence is included in these parts of the table. It can, however, usually be identified optically in non-pseudomorphic textures and fibre veins, so mention of it is omitted from these sections.

**Lizardite usually occurs as the IT Polytype, and occasionally there are minor amounts of a 2H polytype. The occurrence of other multilayer lizardite is specifically noted in the table.

APPENDIX II

ELECTRON MICROPROBE ANALYSES

The mineral analyses were obtained using the fully automated JEOL JX5A electron microprobe at the Geology Department, University of Melbourne. The accelerating voltage was 20 kV, the specimen current 0.02 - 0.03 μA and the beam diameter 5-10 microns. Accuracy for the major elements is $\pm$ 2-5% of amounts tabulated whereas that for minor elements is less than $\pm$ 9% of given values.

APPENDIX III ELECTRON MICROPROBE ANALYSES OF MINERALS FROM THE TENTH LEGION SKARN

	OLIVINE			PYROXENE						AMPHIBOLE
ANALYSIS NO.	1	2	3	4	5	6	7	8	9	10
Sample No.	2-123.65	7-37.2	7-37.2	6-61.65	6-61.65	6-61.65	7-37.2	11-59.2	13-70.6	7-37.2
SiO_2	41.90	40.61	40.68	55.60	54.46	55.16	54.10	54.68	55.09	54.12
TiO_2	-	-	0.01	0.01	0.01	0.01	-	0.03	-	-
Al_2O_3	-	0.01	-	0.03	0.56	0.16	0.12	0.43	0.03	0.05
FeO	5.23	5.42	4.95	0.56	7.92	2.20	1.64	2.32	1.15	1.87
MnO	1.45	1.94	1.74	0.01	0.28	0.34	0.53	0.19	0.33	-
MgO	52.24	51.24	51.48	18.10	15.10	16.78	17.73	16.79	17.73	17.62
CaO	0.02	0.08	0.42	25.59	20.50	24.74	24.91	25.49	24.70	24.81
Na_2O	-	0.04	0.06	0.05	0.13	0.03	0.09	0.08	-	0.04
K_2O	-	-	-	0.04	0.02	-	0.03	0.03	-	0.02
CuO	-	0.02	-	-	-	-	-	0.01	-	-
WO_3	-	-	0.03	-	-	-	-	-	-	-
ZnO	0.02	0.03	0.01	0.08	-	0.01	0.06	0.03	0.01	-
SnO2	-	0.02	-	-	-	-	-	-	-	-
F	-	-	-	-	-	-	-	-	-	-
Cl	-	-	-	-	-	-	0.13	-	-	-
$+H_2O$	-	-	-	-	-	-	-	-	-	2.72
TOTAL	100.89	99.4	99.37	100.17	98.99	100.48	99.34	100.08	99.04	100.64
*Si	1.002	0.991	0.991	2.007	2.025	2.015	1.985	1.992	2.011	7.647
Ti	-	-	-	-	-	-	-	0.001	-	-
Al^{2+}	-	-	-	0.001	0.025	0.007	0.005	0.019	0.001	0.008
Fe^{2+}	0.105	0.111	0.101	0.017	0.255	0.067	0.050	0.071	0.035	0.221
Mn	0.029	0.040	0.036	-	0.009	0.011	0.017	0.006	0.010	-
Mg	1.862	1.864	1.869	0.974	0.837	0.913	0.969	0.912	0.965	3.711
Ca	0.03	0.002	0.011	0.990	0.817	0.968	0.979	0.995	0.966	3.757
Na	-	0.001	0.003	0.004	0.009	0.002	0.006	0.006	-	0.010
K	-	-	-	0.002	0.001	-	0.001	0.001	-	0.003
Cu	-	-	-	-	-	-	-	-	-	-
W	-	-	-	-	-	-	-	-	-	-
Zn	-	0.001	-	-	-	-	-	-	-	-
Sn	-	-	-	-	-	-	-	-	-	-
Cl	-	-	-	-	-	-	-	-	-	-
TOTAL	2.998	3.010	3.010	3.995	3.969	3.983	4.012	4.003	3.988	17.356

* Based on 4 oxygens for olivine, 6 oxygens for pyroxene and 24 oxygens + 2OH for amphibole
\+ Calculated from structural formula.

APPENDIX III Cont'd.

	AMPHIBOLE			SERPENTINE		MICA		CHLORITE	PLAGIOCLASE	GARNET
ANALYSIS No.	11	12	13	14	15	16	17	18	19	20
Sample No.	7-37.2	14-159.65	14-159.65	7-37.2	7-37.2	2-123.65	4-28	2-123.65	11-59.2	14-159.65
SiO_2	52.22	37.29	37.01	40.40	40.61	40.49	42.02	35.54	50.30	39.52
TiO_2	-	0.27	0.20	-	-	0.46	0.08	0.03	-	0.12
Al_2O_3	0.02	12.31	12.12	-	0.01	16.03	13.42	15.55	30.55	18.21
FeO	0.83	26.67	27.03	0.97	2.16	2.69	3.45	2.32	0.44	5.22
MnO	0.36	0.50	0.30	0.14	0.38	0.09	0.13	0.07	0.01	1.12
MgO	17.60	4.62	4.12	39.46	39.91	24.98	25.62	33.50	0.11	0.51
CaO	26.33	11.40	11.23	0.38	0.31	-	-	-	13.59	34.69
Na_2O	0.03	1.67	1.30	0.05	0.03	0.23	0.05	0.02	3.64	-
K_2O	0.02	2.50	2.91	0.04	0.01	10.10	9.53	1.43	0.28	0.01
CuO	-	-	-	-	-	-	-	-	0.01	-
WO_3	-	0.01	-	-	-	-	0.03	-	0.07	-
ZnO	0.02	-	0.10	-	-	0.02	-	-	0.06	-
SnO_2	0.01	0.03	0.03	-	0.01	0.04	-	-	-	-
F	0.02	-	0.05	-	-	-	1.94	-	-	-
Cl	0.05	1.88	2.48	0.04	0.14	0.04	0.05	-	0.01	-
$+H_2O$	2.07	1.37	1.17			4.25	3.30			
TOTAL	99.58	100.51	100.06	81.48	83.58	99.43	99.62	88.46	99.07	99.41
*Si	7.507	6.048	6.080	4.010	3.967	5.699	5.956	6.570	9.276	6.133
Ti	-	0.032	0.025	-	-	0.049	0.009	0.004	-	0.014
Al	0.004	2.354	2.348	-	0.001	2.660	2.242	3.388	6.642	3.330
Fe^{2+}	0.100	3.618	3.713	0.081	0.176	0.317	0.409	0.370	0.068	0.671
Mn	0.044	0.069	0.042	0.012	0.031	0.011	0.015	9.230	0.002	0.147
Mg	3.772	1.117	1.009	5.838	5.810	5.242	5.413	-	0.031	0.118
Ca	4.056	1.981	1.977	0.041	0.032	-	-	0.007	2.687	5.767
Na	0.007	0.525	0.414	0.010	0.006	0.063	0.014	0.337	1.301	-
K	0.003	0.517	0.611	0.005	0.001	1.814	1.723	-	0.065	0.002
Cu	-	-	-	-	-	-	-	-	0.002	-
W	-	-	-	-	-	-	0.001	-	0.004	-
Zn	0.002	-	0.012	-	-	0.002	-	-	0.008	-
Sn	-	0.002	0.002	-	-	0.002	-	-	-	-
F	0.007	-	0.026	-	-	-	0.871	-	-	-
Cl	0.012	0.518	0.690	0.007	0.024	0.011	0.013	-	0.002	-
TOTAL	17.496	18.264	18.233	10.003	10.057	19.860	19.782	19.906	20.088	16.182

* Based on 24 oxygens and 20H for amphiboles; 14 oxygens for serpentine; 24 oxygens and 40H for mica; 36 oxygens and 160H for chlorite; 32 oxygens for plagioclase; 24 oxygens for garnet.

\+ Calculated from structural formulae.

APPENDIX III Cont'd. ELECTRON MICROPROBE ANALYSES (WITH SLIGHTLY LOW TOTALS) OF MINERALS FROM THE TENTH LEGION SKARN

	PYROXENE		CHLORITE		GARNET			SPHENE		
ANALYSIS No.	21	22	23	24	25	26	27	28	29	30
Sample No.	6-61.65	13-70.6	2-123.65	2-123.65	6-55.6	13-70.6	14-159.65	11-59.2	11-59.2	14-159.65
SiO_2	54.69	54.54	30.08	30.34	30.70	36.04	39.52	31.15	30.24	30.36
TiO_2	0.01	-	0.01	0.04	-	-	0.27	30.82	36.53	34.98
Al_2O_3	0.09	0.05	20.48	20.75	0.01	0.12	18.04	2.16	1.79	2.05
FeO	0.82	2.20	3.15	3.03	27.95	27.85	5.39	1.26	0.16	0.61
MnO	0.07	0.34	0.01	0.10	1.00	1.00	1.02	0.07	-	-
MgO	17.72	16.78	30.92	31.27	-	-	0.54	1.89	-	0.01
CaO	25.09	24.74	-	0.02	25.93	32.36	34.36	27.12	28.38	28.68
Na_2O	0.02	0.03	0.02	-	-	0.04	0.02	-	0.02	-
K_2O	-	-	-	0.01	-	-	-	0.04	-	-
CuO	-	-	-	-	-	-	-	-	-	-
WO_3	-	-	-	-	-	-	-	-	-	-
ZnO	-	-	0.07	0.06	-	-	-	-	-	-
SnO_2	0.02	-	-	-	-	-	-	0.02	-	0.53
F	-	-	-	-	-	-	-	-	-	-
Cl	-	-	-	-	-	-	-	0.05	-	-
$+H_2O$			12.45	12.57						
TOTAL	98.54	98.69	97.28	98.19	85.60	97.40	98.71	94.59	97.13	97.22
*Si	2.006	2.010	5.799	5.790	6.497	6.596	6.145	4.174	3.954	3.995
Ti	-	-	0.001	0.006	-	-	0.032	3.106	3.592	3.461
Al	0.004	0.002	4.652	4.667	0.003	0.026	3.306	0.341	0.276	0.318
Fe^{2+}	0.025	0.068	0.507	0.484	4.946	4.262	0.701	0.141	0.018	0.067
Mn	0.002	0.011	0.016	0.017	0.179	0.155	0.134	0.008	-	-
Mg	0.969	0.922	8.885	8.895	-	-	0.125	0.378	-	0.002
Ca	0.986	0.977	-	0.003	5.879	6.345	5.724	3.893	3.975	4.043
Na	0.001	0.002	0.006	-	-	0.014	0.006	-	0.005	-
K	-	-	0.001	0.002	-	-	-	0.007	-	-
Cu	-	-	-	-	-	-	-	-	-	-
W	-	-	-	-	-	-	-	-	-	-
Zn	-	-	0.009	0.008	-	-	-	-	-	-
Sn	-	-	-	-	-	-	-	-	-	-
F	-	-	-	-	-	-	-	-	-	-
Cl	-	-	-	-	-	-	-	0.011	-	-
TOTAL	3.993	3.992	35.878	35.872	17.504	17.398	16.173	12.059	11.820	11.886

* Based on 6 oxygens for pyroxene; 36 oxygens and 16OH for chlorite; 24 oxygens for garnet; 20 oxygens and 1OH for sphene.

\+ Calculated from structural formulae.

APPENDIX III (cont'd.)

	EPIDOTE		
ANALYSIS NO.	31	32	33
Sample No.	14-159.65	14-159.65	14-159.65
SiO_2	37.48	38.13	38.16
TiO_2	-	-	0.04
Al_2O_3	21.87	23.27	24.55
FeO	13.17	11.21	10.70
MnO	0.28	0.33	0.10
MgO	0.02	0.04	0.02
CaO	21.83	22.23	23.10
Na_2O	0.01	-	-
K_2O	-	-	-
CuO	-	-	-
WO_3	-	0.01	0.01
ZnO	-	-	-
SnO_2	-	-	0.07
F	-	-	-
Cl	-	-	-
H_2O			
TOTAL	94.68	95.23	96.78
*Si	3.159	3.158	3.106
Ti	-	-	0.002
Al^{2+}	2.173	2.271	2.355
Fe	0.928	0.776	0.728
Mn	0.020	0.023	0.007
Mg	0.003	0.005	0.002
Ca	1.971	1.973	2.014
Na	0.002	-	-
K	-	-	-
Cu	-	-	-
W	-	-	-
Zn	-	-	-
Sn	-	-	-
F	-	-	-
Cl	-	-	-
TOTAL	8.256	8.206	8.214

* Based on 13 oxygens and 1OH for epidote.

+ Calculated from structural formulae.


4900E.
4940E.
5000E.
50M/75
DATUM POINT 4990N. 5000E. GRID
D.D.82T.L.C11
D.D.82T.L.C10
D.D.82T.L.C14
D.D.81T.L.C9
D.D.81T.L.C1
D.D.81T.L.C2
Mines Dept. Nº2
Adit Nº1
Adit Nº3
Adit Nº2
Adit Nº4
? possible mag. o/c?
? Oonah Quartzite
PINE CREEK
Old Adit
4990 N.
5100E.
5200E.
5300E.
5400E.
5500E.
5600E.
5700E.
5750E.
D.D.H. in track
D.D.82 T.L.C12
53M/75
Tr. Py in soil
Creek py. mag.
Massive magnetite and altered sediments on dump.
Dump
D.D.82 T.L.C13
Note: Creek drains Silver Stream – Kynance workings
Rounded lag? qtz. qtzite
qtzite float (lag?)
Old track qtzite float
5280E.
qtzite float (lag)
Laterite
Laterite capping
D.D.81 T.L.C6
5680E.
5780E.
5880E.
5980E.
6080E.
4250 N.
MOSTLY COVERED BY LATERITE
Adit dump magnetite qtz-epidote rock on dump.
Magnetite capping
? collapsed costean
Mn rich laterite capping on green calc-silicate with dissem. mag.
Trench
D.D.81 T.L.C7
Manganiferous gossan float
52M/75
54M/75
Sulphidic gossanous zone in calc-silicates (py, gn, sp, cp.)
Gossanous and magniferous zone
Gossanous float with much manganese
KYNANCE CREEK
2m Shaft
6m Shaft
5445E.
3850 N.
51M/75
4700E.
4800E. (4778.5E ON BASELINE)
5000E. (4982E ON BASELINE)
5200E. (5181.7E ON BASELINE)
Small prospecting pit green-grey calc-silicates with finely diss. py.
Mn rich capping with limonite minor mag.
Mn rich capping and float
8m Shaft
T.M.I. D.D.H.
Shaft in magnetite ± brown clay
D.D.81 T.L.C8
D.D.81 T.L.C3
Gabbro o/c. in track
D.D.81 T.L.C4
min. o/c with mag. sp.
sp, green mica
Adits and trenches
D.D.81 T.L.C5
o/c with 5-15% py, po
Calc-silicate with minor mag. py.
3105 N.
067
LEGEND
QUATERNARY
a Recent cover (mainly button grass swamp)
m Magnetite scree; lateritic ferruginous capping and scree.
CAMBRIAN - UPPER PROTEROZOIC
Ls Dolomitic Limestone
Impure partially serpentinised carbonate sequence, variably altered to Calc - Silicate sequence, below.
Cs Calc - Silicate Sequence
Predominantly hard calc - silicates after altered hornfelsed impure carbonate sediments. Also serpentinite, dolomite, cherts and hornfelsed tourmalinitic siltstone
M Magnetite
Usually massive, often with lateritic capping.
Ss Siltstones and Shales
Grey siltstones and phyllitic sericitic grey shales. Minor impure quartzite. Generally soft and clayey.
Oq Oonah Quartzite
Impure quartzite; quartzose sandstones and siltstones; grey shales. Some quartz - tourmaline veining.
IGNEOUS ROCKS
G Gabbro
415068
5 cm
SCALE 1:2500
0 25 50 75 100 Metres
C.R.A. EXPLORATION PTY. LIMITED
TENTH LEGION PROSPECT
WESTERN TASMANIA
INTERPRETIVE GEOLOGY AND DIAMOND DRILL PLAN
geologist: G.B.
scale: 1:2500
report no: 11732
drawn: T.G.D.S.
date: June 1982
plan no: TAS.h 86

068

415069

Fig. 2 Simplified cross-section of northern drill holes (1-12)

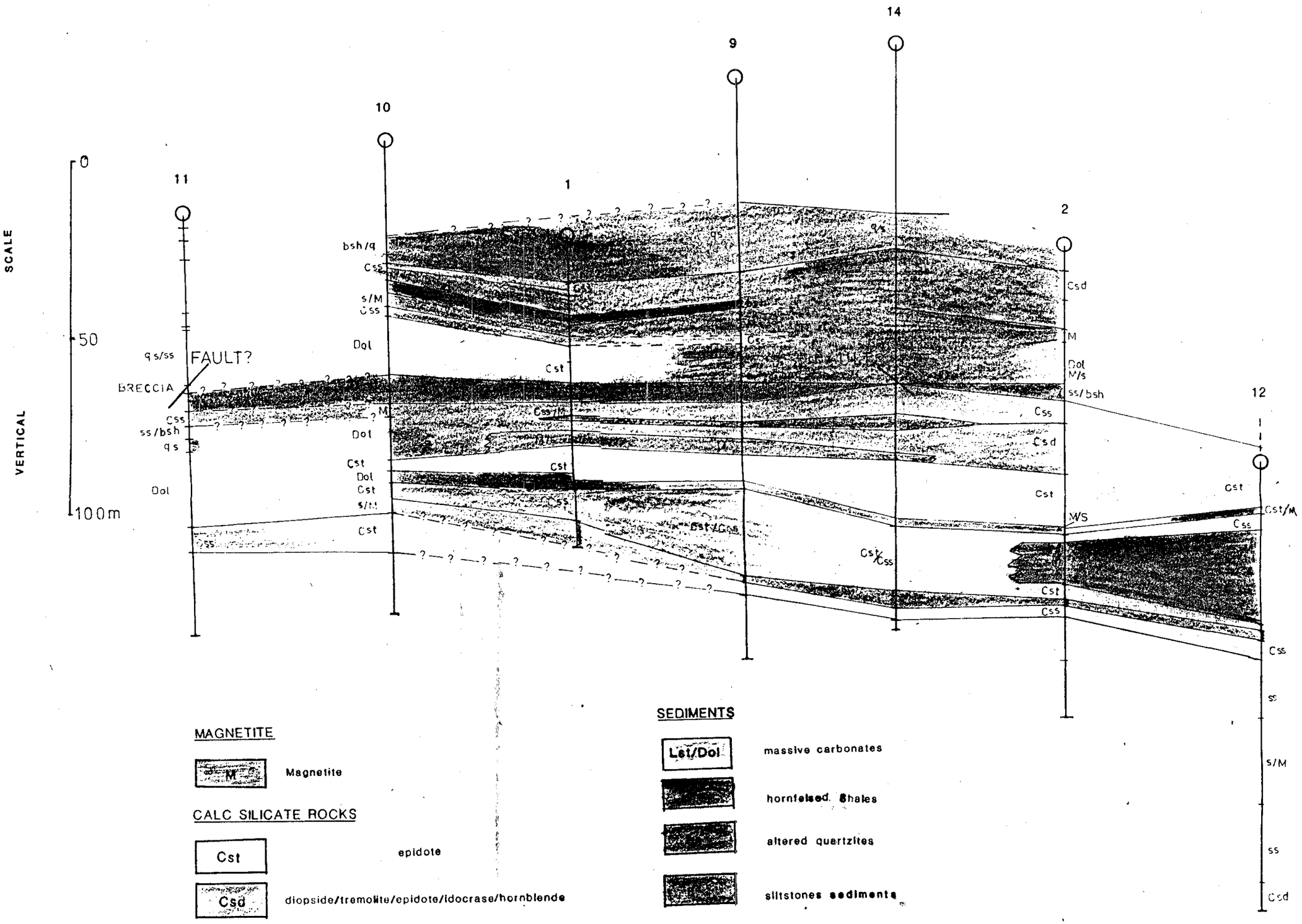

MAGNETITE

M — Magnetite

CALC SILICATE ROCKS

Cst — epidote

Csd — diopside/tremolite/epidote/idocrase/hornblende

Css — hybrid skarn either of the above

S — serpentine

SEDIMENTS

Lst/Dol — massive carbonates

hornfelsed shales

altered quartzites

siltstones sediments

Compiled from C.R.A.E drill sections

Thomson'83.